Loop-induced neutrino masses: A case study

Chao-Qiang Geng,[*] Da Huang,[†] and Lu-Hsing Tsai[‡]

Chongqing University of Posts & Telecommunications, Chongqing, 400065, China; Department of Physics, National Tsing Hua University, Hsinchu 300, Taiwan and Physics Division, National Center for Theoretical Sciences, Hsinchu 300, Taiwan

(Received 4 October 2014; published 8 December 2014)

We study the cocktail model in which the Majorana neutrino masses are generated by the so-called "cocktail" three-loop diagrams with the dark matter particle running in the loops. In particular, we give the analytic expressions of the neutrino masses in the model by the detailed calculation of the cocktail diagrams. Based on the numerical calculation of the loop integrals, we explore the parameter space which can give the correct orders of neutrino masses while satisfying other experimental constraints, such as those from the neutrinoless double beta decay, low-energy lepton flavor violation processes, electroweak precision tests, and collider searches. As a result, the large couplings and the large mass difference between the two singly charged (neutral) scalars are required.

DOI: 10.1103/PhysRevD.90.113005 PACS numbers: 14.60.Pq, 12.60.Fr, 95.35.+d

I. INTRODUCTION

The small but nonzero masses and mixings of the neutrinos have been found via the neutrino oscillation experiments [1], while dark matter (DM) has been established by astrophysical observations [2–4]. Both phenomena cannot be explained within the Standard Model (SM) of particle physics, directly pointing to the existence of new physics.

One possible explanation of the tiny neutrino masses is the canonical seesaw mechanisms, where the masses are generated at tree level by introducing right-handed neutrinos [5] or a Higgs triplet [6] or fermion triplets [7]. Unfortunately, such new particles are predicted too heavy to be studied at the current colliders. Another idea is to promote the neutrino mass generation to loop levels [8], where the smallness of the neutrino masses is attributed to the loop suppression and the masses of the new particles are naturally of $\mathcal{O}(100\text{–}1000)$ GeV or even smaller so that the phenomenology can be very rich. In particular, the discrete symmetries imposed on some models play an extra role to guarantee the stability of DM [9], resulting in a common origin of neutrino masses and DM. The cocktail model [10] is one recent example along this line of thinking, in which the Majorana neutrino mass terms first appear at three-loop level via the so-called "cocktail" diagrams, while DM is identified as a neutral Z_2-odd particle running in the loops. It is interesting to note that the model naturally predicts the normal hierarchy form of the neutrino mass matrix.

However, the detailed derivations of the formula for the neutrino masses from the cocktail diagrams were not given in Ref. [10]. In this paper, we present the full form of the neutrino mass formula in this model. Moreover, with the explicit analytic calculation of the relevant Feynman diagrams and the numerical integration, we explore the parameter space which can give the required values of the neutrino masses while satisfying all of the other constraints from the neutrinoless double beta ($0\nu\beta\beta$) decay, low-energy lepton flavor violation (LFV) processes, electroweak precision tests (EWPTs), and collider searches.

The paper is organized as follows. In Sec. II, we show the particle content in the cocktail model and the relevant part of the Lagrangian. In Sec. III, we examine the neutrino mass matrix by considering the current neutrino oscillation data and the $0\nu\beta\beta$ constraint. We then discuss the constraints from LFV processes, EWPTs, and DM and collider searches in Secs. IV, V, and VI, respectively. Our numerical exploration of the parameter space is carried on in Sec. VII. A short summary is given in Sec. VIII. In the Appendix, the analytical calculation details of the cocktail diagrams are presented.

II. THE COCKTAIL MODEL FOR NEUTRINO MASSES

Besides the SM fields and symmetries, two $SU(2)_L$ singlet scalars, S^+ and ρ^{++}, and a scalar doublet Φ_2 are introduced, and an exact Z_2 symmetry is imposed. Under Z_2, S^+ and Φ_2 are odd, while ρ^{++} and all the SM fields are even. After the electroweak (EW) symmetry breaking, the Z_2 symmetry keeps so that the lightest Z_2-odd state remains stable and becomes a DM particle candidate. The particle content of the new physics sector is summarized in Table I, and the relevant Lagrangian is given by

[*]geng@phys.nthu.edu.tw
[†]dahuang@phys.nthu.edu.tw
[‡]lhtsai@phys.nthu.edu.tw

TABLE I. New physics sector particle content of the cocktail model.

	$SU(2)_L$	$U(1)_Y$	Z_2
Φ_2	**2**	1	−
S^+	**1**	2	−
ρ^{++}	**1**	4	+

$$-\mathcal{L}_{\rm dark} = \frac{\lambda_5}{2}(\Phi_1^\dagger\Phi_2)^2 + \kappa_1\Phi_2^T i\sigma_2\Phi_1 S^- + \kappa_2\rho^{++}S^-S^- + \xi\Phi_2^T i\sigma_2\Phi_1 S^+\rho^{--} + C_{ab}\bar{\ell}^c{}_{aR}\ell_{bR}\rho^{++} + \text{H.c.}, \quad (1)$$

where a and b denote the three families of the right-handed leptons ℓ_R, and C_{ab} are the elements of the Yukawa coupling matrix which is symmetric and complex in general.

After the spontaneous breaking of the EW symmetry, the SM Higgs doublet Φ_1 and inert scalar doublet Φ_2 can be written in the unitary gauge as

$$\Phi_1 = \begin{pmatrix} 0 \\ v + \frac{h}{\sqrt{2}} \end{pmatrix}, \qquad \Phi_2 = \begin{pmatrix} \Lambda^+ \\ \frac{1}{\sqrt{2}}(H_0 + iA_0) \end{pmatrix}, \quad (2)$$

where $v \approx 174$ GeV is the vacuum expectation value (VEV) of the SM Higgs Φ_1. With a nonzero κ_1, the charged scalars Λ^+ and S^+ will mix together with an angle β, leading to two charged mass eigenstates

$$H_1^+ = s_\beta S^+ + c_\beta \Lambda^+, \qquad H_2^+ = c_\beta S^+ - s_\beta \Lambda^+, \quad (3)$$

with $s_\beta(c_\beta) = \sin\beta(\cos\beta)$. In the mass eigenstate basis, the most useful set of independent variables is the five new scalar masses $m_{\rho,H_0,A_0,H_{1,2}^+}$, the mixing angle β, and the couplings ξ and κ_2. All the original parameters defined in the scalar potential in Eq. (1) can be solved with these physical parameters.

The lepton number is explicitly broken in the Lagrangian of Eq. (1) by two units, which is the necessary condition to generate the Majorana masses for the three light active neutrinos. However, as pointed out in Ref. [10], the leading contribution to the neutrino masses appears at three-loop level via the so-called "cocktail diagrams" shown in Fig. 1.

In the basis where the charged leptons are in mass eigenstates and the charged current interactions are flavor diagonal, the Majorana neutrino mass matrix elements are given by

$$(m_\nu)_{ab} = (x_a C_{ab} x_b)\frac{s_{2\beta}}{(16\pi^2)^3}(\mathcal{A}_1\mathcal{I}_1 + \mathcal{A}_2\mathcal{I}_2), \quad (4)$$

with

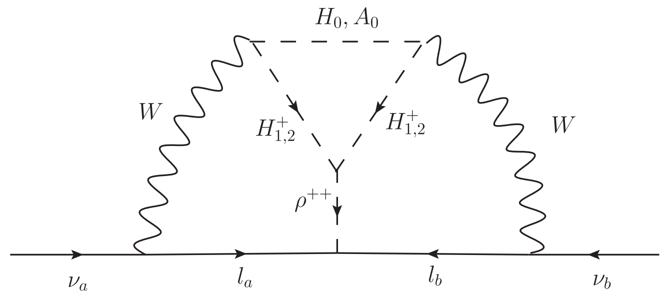

FIG. 1. Cocktail diagrams for neutrino masses.

$$\mathcal{A}_1 = \frac{[\kappa_2 s_{2\beta} + (\xi v)c_{2\beta}]}{m_\rho^2}\frac{(\Delta m_+^2)^2\Delta m_0^2}{m_\rho^2 v^2},$$
$$\mathcal{A}_2 = \frac{\xi v}{m_\rho^2}\frac{\Delta m_+^2 \Delta m_0^2}{v^2}, \quad (5)$$

where m_ρ denotes the mass of the doubly charged scalar ρ^{++}, $x_i = m_i/v$ $(i = a, b)$, $\Delta m_+^2 = m_{H_1^+}^2 - m_{H_2^+}^2$, and $\Delta m_0^2 = m_{H_0}^2 - m_{A_0}^2$. Note that the powers of m_ρ in the denominators in Eq. (5) are just to make the integrals $\mathcal{I}_{1,2}$ dimensionless for convenience, rather than their actual scaling dimensions. The details of the derivations of Eqs. (4) and (5) as well as the precise definitions of the dimensionless integrals $\mathcal{I}_{1,2}$ are contained in Appendix A. In our work, we have applied different widely used softwares and packages to reliably perform the numerical integration of $\mathcal{I}_{1,2}$, such as MATHEMATICA, SECDEC [11], and GSL [12]. As a result, we find that the benchmark point given in the first version of Ref. [10] before its erratum generically predicts the neutrino masses typically about 2 orders smaller than the measured ones, no matter what value of the coupling ξ is if it is within the perturbative region $\xi \le 5$ [13], which is also discussed in detail in the Appendix.

It should be mentioned that the neutrino masses in Eq. (4) are proportional to $s_{2\beta}$. With our numerical studies, we conclude that the neutrino masses are usually insufficient to explain the oscillation data in most parameter spaces except those with large couplings κ_2 and ξ and large mass splittings Δm_+^2 and Δm_0^2. In order not to introduce an extra suppression, we take the maximum value of $s_{2\beta} = 1$, i.e., $\beta = \pi/4$ in our following discussions.

III. NEUTRINO MASS MATRIX

Currently, the mass differences and the mixings among three active neutrinos are measured to a very high precision, with the recent worldwide best-fit values as follows [14]:

$$\Delta m^2_{\rm sun} = (7.54^{+0.26}_{-0.22}) \times 10^{-5}\ \text{eV}^2,$$
$$|\Delta m^2_{\rm atm}| = (2.43^{+0.06}_{-0.06}) \times 10^{-3}\ \text{eV}^2,$$
$$\sin^2\theta_{12} = 0.308 \pm 0.017, \qquad \sin^2\theta_{23} = 0.437^{+0.033}_{-0.023},$$
$$\sin^2\theta_{13} = 0.0234^{+0.0020}_{-0.0019}. \quad (6)$$

The remaining questions are the pattern of the neutrino mass hierarchy and the four undetermined parameters: the smallest neutrino mass m_0 and three CP violating phases, δ (Dirac) and $\alpha_{21,31}$ (Majorana), in the standard parametrization of the neutrino mixing matrix (see Ref. [14]).

To investigate the above questions in the context of the cocktail model, let us begin our discussion by noticing that the form of the neutrino mass matrix, that is, the relative size of each element, is determined by the Yukawa couplings C_{ab}. If all C_{ab} are assumed to be of $\mathcal{O}(1)$, it is generically expected that the neutrino mass matrix should be in the form of the normal hierarchy since the mass elements are proportional to $x_a x_b$. And the elements $(m_\nu)_{ee,e\mu}$ should be much smaller than others due to the hierarchy $x_e \ll x_\mu \ll x_\tau$. With this expectation, we focus on the parameter space in which $(m_\nu)_{ee,e\mu}$ are approximately zero compared to other elements. This restriction amounts to four constraints to the active neutrino mass matrix, fixing the four known parameters to be

$$m_0 = 5.14 \times 10^{-3}\ \text{eV}, \qquad \delta = 1.89, \qquad \alpha_{21} = 2.80, \qquad \alpha_{31} = 1.67. \tag{7}$$

Consequently, the neutrino mass matrix can be predicted as

$$m_\nu = \begin{pmatrix} \approx 0 & \approx 0 & 10.1 \\ \approx 0 & -5.01 & 0.0980 \\ 10.1 & 0.0980 & -4.77 \end{pmatrix} \times 10^{-3} + i \begin{pmatrix} \approx 0 & \approx 0 & 0.23 \\ \approx 0 & -2.37 & -2.33 \\ 0.23 & -2.33 & -2.74 \end{pmatrix} \times 10^{-2}\ \text{eV}, \tag{8}$$

where we have only used the central values in Eq. (6). Note that $(m_\nu)_{ee,e\mu}$ are very sensitive to the choice of m_0 and the CP phases, so that if we keep $(m_\nu)_{ee,e\mu}$ small enough, the unknown parameters and the resulted neutrino masses cannot deviate the benchmark in Eqs. (7) and (8) much.

With Eq. (8) and the formula for the cocktail model in Eq. (4), we can determine the Yukawa coupling matrix up to only one unknown parameter $|C_{e\tau}|$, given by

$$C_{ab} = \begin{pmatrix} \leq \mathcal{O}(10^{-2}) & \leq \mathcal{O}(10^{-2}) & e^{0.224i} \\ \leq \mathcal{O}(10^{-2}) & 1.90 \times 10^{-1} e^{-1.78i} & 1.08 \times 10^{-2} e^{-1.56i} \\ e^{0.224i} & 1.08 \times 10^{-2} e^{-1.56i} & 7.73 \times 10^{-4} e^{-1.74i} \end{pmatrix} \times |C_{e\tau}|. \tag{9}$$

We will take advantage of this rigid structure of the Yukawa coupling matrix in our discussion of LFV processes by expressing their constraints in terms of $|C_{e\tau}|$. Note that the elements $C_{ee,e\mu}$ cannot be determined with the benchmark point in Eq. (8). Actually, they can be tuned to be as small as possible without affecting the neutrino mass matrix form. The largest orders shown in Eq. (9) are obtained by combining the constraints from the $0\nu\beta\beta$ decay and LFV processes.

The neutrinoless double beta decay, as a lepton number violating process, should exist with a nonzero $(m_\nu)_{ee}$, which is equivalent to a nonzero C_{ee} in the cocktail model. In the conventional neutrino mass generation models, such as the type-II seesaw model [6], the long-distance contribution as shown in Fig. 2(a) dominates the decay process, while for the cocktail model models which can generate the effective coupling $\rho^{--} W^+_\mu W^{\mu+}$, the short-distance channel shown in Fig. 2(b) gives the contribution several orders larger than the long-distance one [15–19]. This feature can be traced to the fact that the amplitude of Fig. 2(b) is proportional to C_{ee}, rather than m_{ee}, which is further suppressed by the small

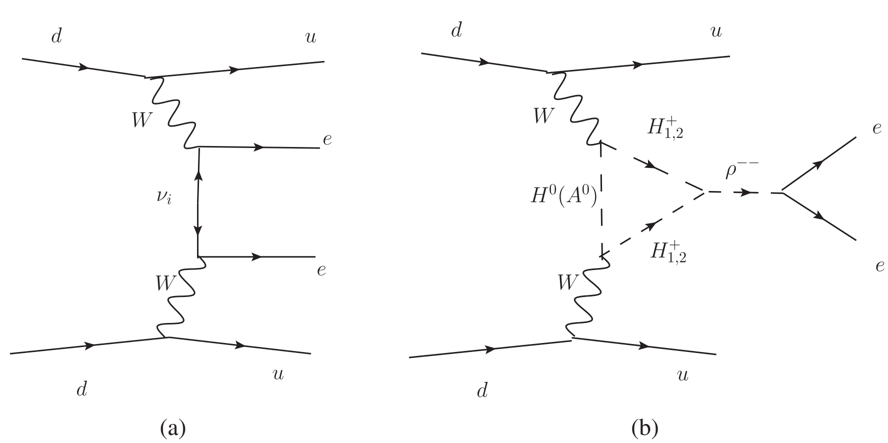

FIG. 2. $0\nu\beta\beta$ decay from (a) long-distance and (b) short-distance diagrams.

TABLE II. G_{01} (in unit 10^{-14} yr^{-1}) and $|\mathcal{M}_3|$ for different nuclei, where the numerical values are taken from Ref. [16].

	^{76}Ge	^{136}Xe	^{150}Nd	^{130}Te	^{82}Se	^{100}Mo
G_{01}	0.640	4.73	21.0	4.44	2.82	4.58
$\|\mathcal{M}_3\|$	209	107	305	193	188	241

electron mass squared m_e^2. In this way, some parameter spaces have already been probed and constrained by the current $0\nu\beta\beta$ experiments. Since the energy transfer in the $0\nu\beta\beta$ decay is only of order 100 MeV, the short-distance contribution in Fig. 2(b) to the half-life for the $0\nu\beta\beta$ decay in the cocktail model can be expressed by [18]

$$T_{1/2}^{\nu 0\beta\beta} = [4m_p^2 G_{01}|\mathcal{A}|^2|\mathcal{M}_3|^2]^{-1}, \tag{10}$$

where m_p is the mass of the proton, G_{01} the phase space factor,

$$\begin{aligned}\mathcal{A} = \frac{C_{ee}s_{2\beta}\Delta m_+^2}{8\pi^2 m_\rho^2}\{&[\kappa_2\Delta m_+^2 s_{2\beta} - \xi v(c_\beta^2 m_{H_2}^2 + s_\beta^2 m_{H_1}^2)]\\ &\times[F_{H_1^+,H_2^+,H_0} - F_{H_1^+,H_2^+,H_0}]\\ &- \xi v[m_{H_0}^2 F_{H_1^+,H_2^+,A_0} - m_{A_0}^2 F_{H_1^+,H_2^+,A_0}]\},\end{aligned} \tag{11}$$

with

$$F_{a,b,c} = \int_0^1 du \int_0^1 dv \times \frac{u^3 v(1-v)}{[uvm_a^2 + u(1-v)m_b^2 + (1-u-v)m_c^2]^2}, \tag{12}$$

and $\mathcal{M}_3$ the nuclear matrix element enveloping the operator $\bar{u}_L\gamma^\mu d_L \bar{u}_L\gamma_\mu d_L \bar{e}_R e_R^c$, as defined in Refs. [16,20,21]. The numerical values of G_{01} and $\mathcal{M}_3$ for several conventional targets are collected in Table II [16].

For a rough estimation, we take a benchmark point for the scalar masses and related coupling constants as an illustration, given by $\kappa_2 = 6$ TeV, $\xi = 5$, $m_{H_1} = 200$ GeV, $m_{H_2} = 720$ GeV, $m_{H_0} = 70$ GeV, $m_{A_0} = 430$ GeV, and $m_\rho = 2$ TeV. From the current experimental detections [22–27], we can obtain the upper bound on C_{ee} by applying Eq. (10), with the results listed in Table III. Generically, C_{ee} should be less than 10^{-3} to fulfill all the present experimental constraints with the most tight constraints on C_{ee} from the detections for the targets ^{76}Ge and ^{136}Xe. On the other hand, models with the long-distance dominance usually predict an undetectable half-life for the $0\nu\beta\beta$ decay [18]. Therefore, future experiments with a higher sensitivity [28] could help to distinguish the cocktail model from the conventional ones.

TABLE III. Experimental lower bounds on the half-life of $0\nu\beta\beta$ with the corresponding maximal values of $|C_{ee}|$.

	$> T_{\rm exp}(10^{25}$ yr)	$\|C_{ee}\|_{\max}$
GERDA-1(^{76}Ge) [22]	2.1	0.0015
KamLAND-Zen(^{136}Xe) [23]	1.9	0.0011
NEMO-3(^{150}Nd) [24]	0.0018	0.0060
CUORICINO(^{130}Te) [25]	0.3	0.0016
NEMO-3(^{82}Se) [26,27]	0.036	0.0059
NEMO-3(^{100}Mo) [27]	0.11	0.0021

IV. FLAVOR CONSTRAINTS

The overall size of the Yukawa coupling matrix in Eq. (9) is mostly constrained by the LFV processes mediated by the doubly charged scalar ρ^{++}, in which the most relevant ones can be categorized into two kinds, $\ell_0^\mp \to \ell_1^\pm \ell_2^\mp \ell_3^\mp$ and $\ell_0^\pm \to \ell_1^\pm\gamma$, and the corresponding formulas are listed as

$$\begin{aligned}\mathcal{B}(\ell_0^\mp \to \ell_1^\pm \ell_2^\mp \ell_3^\mp) &= \frac{|C_{\ell_1\ell_0}C^*_{\ell_2\ell_3}|^2}{2m_\rho^4 G_F^2}\frac{m_{\ell_0}^5}{m_\mu^5}\mathcal{B}(\mu^- \to e^-\bar{\nu}_e\nu_\mu),\\ \mathcal{B}(\ell_0^\pm \to \ell_1^\pm\gamma) &= \frac{\alpha_{\rm em}}{3\pi}\frac{|\sum_\ell C^*_{\ell_1\ell}C_{\ell\ell_0}|^2}{G_F^2 m_\rho^4}\frac{m_{\ell_0}^5}{m_\mu^5}\\ &\quad\times\mathcal{B}(\mu^- \to e^-\bar{\nu}_e\nu_\mu).\end{aligned} \tag{13}$$

With Eq. (13), the bounds on the various LFV processes [14,29,30] can be translated into the ones on the Yukawa couplings:

$$\begin{aligned}
&\mathcal{B}(\mu^+ \to e^+\gamma) < 5.7\times 10^{-13}: && \Big|\sum_\ell C_{\ell\mu}C^*_{\ell e}\Big| < 3.16\times 10^{-4}(m_\rho/\text{TeV})^2,\\
&\mathcal{B}(\mu^- \to 3e) < 1.0\times 10^{-12}: && |C_{e\mu}C^*_{ee}| < 2.33\times 10^{-5}(m_\rho/\text{TeV})^2,\\
&\mathcal{B}(\tau^- \to 3e) < 2.7\times 10^{-8}: && |C_{e\tau}C^*_{ee}| < 9.1\times 10^{-3}(m_\rho/\text{TeV})^2,\\
&\mathcal{B}(\tau^- \to 3\mu) < 2.1\times 10^{-8}: && |C_{\mu\tau}C^*_{\mu\mu}| < 8.0\times 10^{-3}(m_\rho/\text{TeV})^2,\\
&\mathcal{B}(\tau^- \to e^-\mu^+\mu^-) < 2.7\times 10^{-8}: && |C_{\mu\tau}C^*_{e\mu}| < 6.42\times 10^{-3}(m_\rho/\text{TeV})^2,\\
&\mathcal{B}(\tau^- \to \mu^-e^+e^-) < 1.8\times 10^{-8}: && |C_{e\tau}C^*_{e\mu}| < 5.24\times 10^{-3}(m_\rho/\text{TeV})^2,\\
&\mathcal{B}(\tau^- \to e^+\mu^-\mu^-) < 1.7\times 10^{-8}: && |C_{e\tau}C^*_{\mu\mu}| < 7.21\times 10^{-3}(m_\rho/\text{TeV})^2,\\
&\mathcal{B}(\tau^- \to \mu^+e^-e^-) < 1.5\times 10^{-8}: && |C_{\mu\tau}C^*_{ee}| < 6.77\times 10^{-3}(m_\rho/\text{TeV})^2.
\end{aligned} \tag{14}$$

These constraints, together with the typical Yukawa matrix pattern in Eq. (9), can yield the upper bound on the overall size of the Yukawa coupling $|C_{e\tau}| < 0.168(m_\rho/\text{TeV})$, which comes mainly from the process $\mu \to e\gamma$. For the later convenience, we shall take $|C_{e\tau}| = 0.15(m_\rho/\text{TeV})$ in our numerical exploration of the parameter space. For $C_{ee,e\mu}$, the bound on the branching ratio of $\mu \to 3e$ restricts $C_{ee,e\mu} \le \mathcal{O}(10^{-3})$, which are consistent with the aforementioned $0\nu\beta\beta$ decay constraints.

V. ELECTROWEAK PRECISION TEST CONSTRAINTS

Since all of the newly introduced particles carry EW charges, the cocktail model is also well constrained by the EWPTs at the LEP, especially the T parameter [31,32], for which the new one-loop correction is as follows [10]:

$$\Delta T = \frac{1}{16\pi m_W^2 s_W^2}[c_\beta^2(F_{H_1^+,H_0} + F_{H_1^+,A_0}) + s_\beta^2(F_{H_2^+,H_0} + F_{H_2^+,A_0}) - 2c_\beta^2 s_\beta^2 F_{H_1^+,H_2^+} - F_{H_0,A_0}], \quad (15)$$

where

$$F_{i,j} = \frac{m_i^2 + m_j^2}{2} - \frac{m_i^2 m_j^2}{m_i^2 - m_j^2}\ln\frac{m_i^2}{m_j^2}, \quad (16)$$

and s_W (c_W) is the sine (cosine) of the Weinberg angle θ_W. As already pointed in Ref. [10], the cancellation between the charged and neutral states becomes possible, resulting in an extended parameter space. In particular, the present model allows a large mass splitting between the two neutral (charged) particles.

VI. DARK MATTER PHYSICS AND COLLIDER CONSTRAINTS

DM physics and the collider searches have already provided interesting constraints on the cocktail model. Since the cocktail model is very similar to the widely studied inert doublet model (IDM) [33] in the Z_2-odd sector except for the additional singly charged scalar, we would expect that the results about the DM properties in the IDM could be applied directly. In the following, we just summarize some of the relevant conclusions from the most recent global fitting studies in Ref. [34]. Other aspects of the IDM can be referred to Refs. [34–37].

In the cocktail model, there is no preference of the neutral scalar H_0 or the pseudoscalar A_0 to be the dark matter candidate. Thus, without loss of generality, we assume that the lightest Z_2-odd particle is H_0. According to the analysis in Ref. [34], there are two regions, 60 GeV $< m_{H_0} <$ 75 GeV (low mass) and $m_{H_0} >$ 500 GeV (high mass), that can give rise to the correct relic DM density while satisfying all other experimental constraints, including LHC searches, direct detection bounds from LUX and XENON100, and indirect signals from AMS-02 and Fermi-LAT, with the low mass region favored by the fit. In addition, in the large mass region, it is crucial that $m_{H_0} \approx m_{A_0}$, which is required by the coannihilation of the DM H_0 with A_0 to generate the correct DM relics. On the other hand, it is clear from Eqs. (4) and (5) that the right amount of the neutrino masses needs a large enough mass difference between H_0 and A_0. Therefore, there is some tension between the DM relic density and the neutrino masses in the high mass region. In the following, we only focus on the low mass region and take $m_{H_0} =$ 70 GeV as our benchmark point, which is also the best-fitting point in Ref. [34]. In this region, the right relic density in the Universe [3] can be obtained by the combination of three effects [34,35]: the coannihilation among H_0, A_0 and $H_1^\pm$; the SM Higgs resonance enhancement; and the opening of the W^+W^- annihilation channel. Furthermore, if we restrict the coupling $-\lambda_5(\Phi_1^\dagger\Phi_2)^2/2$ to be within the perturbative region with $|\lambda_5| < 5$, we find that the upper bound for the pseudoscalar mass is $m_{H_0} < m_{A_0} <$ 555 GeV. However, the LEP has excluded models with $m_{A_0} \le 100$ GeV when $m_{H_0} = 70$ GeV [38].

The allowed range of the masses for the charged particles are well constrained by the EWPTs, especially the T parameter. Due to the mixing involving with the extra $SU(2)_L$ singlet charged scalar, it is clear that the results in the present cocktail model vastly differ from those in the IDM as shown in Eq. (15), so that we cannot directly copy the conclusion in Ref. [34] here. Rather, if we require the heavier singly charged scalar H_2^+ to be less than 1 TeV and the mass splitting Δm_+^2 large enough to generate measured values of the neutrino masses, $m_{H_1^+}$ should not exceed 500 GeV from our numerical studies. Thus, we take three benchmark points with $m_{H_1^+} = 90$, 200, and 300 GeV, respectively, which are all allowed by the LEP constraints $m_{H_1^+} \le$ 70–90 GeV [39]. Note that the latest 8 TeV ATLAS [40–42] and CMS [43,44] bounds on the chargino and neutralino masses cannot be applied here, since either they assumed the equal mass of the lightest chargino and second-lightest neutralino in the associated production channel [40,41,43,44] or the constraining power on the lightest chargino mass was only confined within the DM masses smaller than about 30 GeV in the chargino pair production one [41]. For the doubly charged scalar ρ^{++}, the most stringent bounds on its mass are 409 and 459 GeV for the ATLAS [45] and CMS [46] 7 TeV data, respectively.

VII. NUMERICAL RESULTS

Instead of the exploration of the whole parameter space, we only present some benchmark points of phenomenological interest. In particular, we focus on the particle spectra in which $m_\rho = 1$ and 2 TeV with $m_{H_1} = 90$, 200, and 300 GeV. If we further confine the couplings (κ_2, ξ)

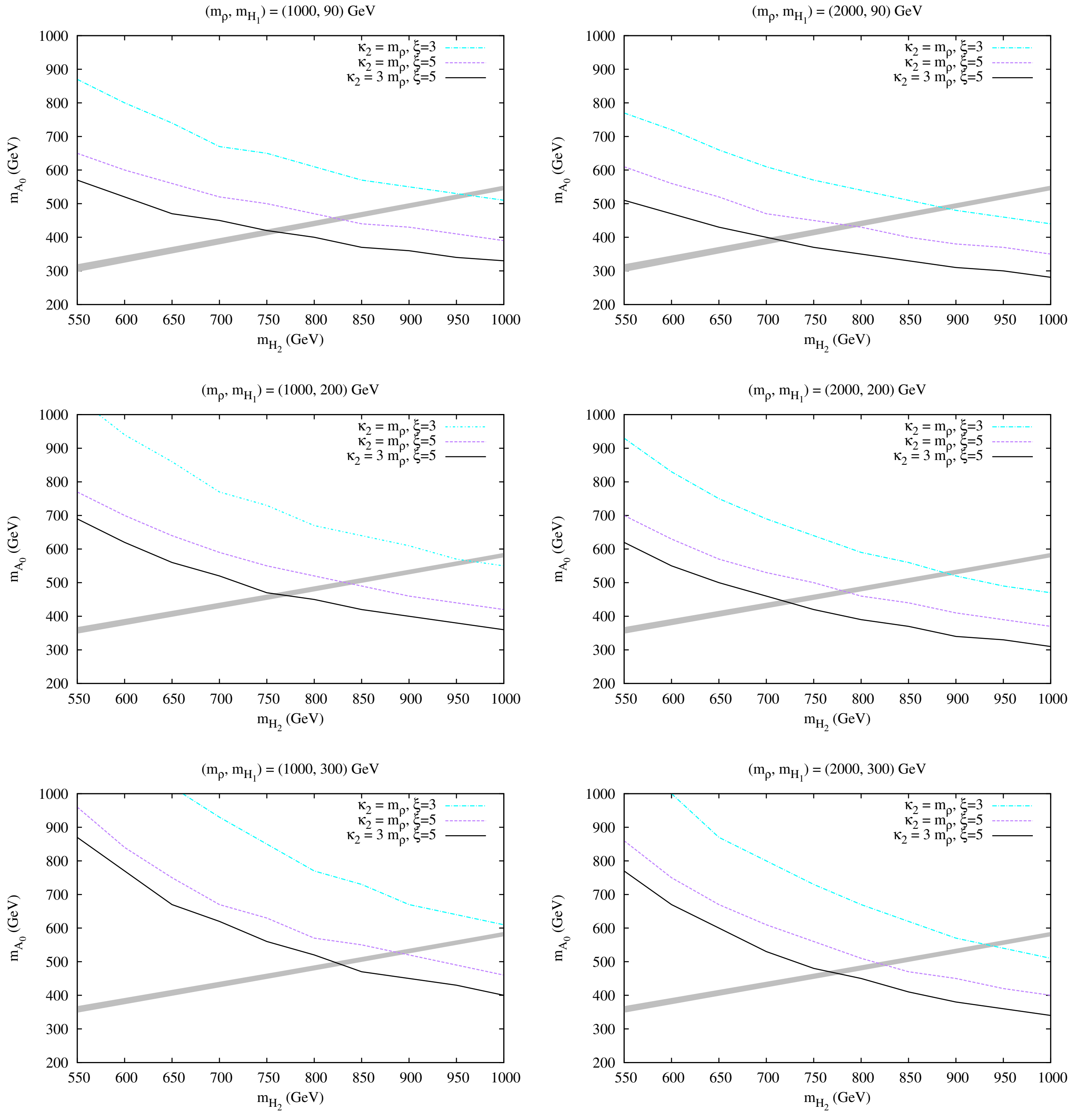

FIG. 3 (color online). Benchmark points for allowed parameter space, where the grey bands represent 1σ errors of the allowed parameter spaces from ΔT.

within the perturbative region and take the following characteristic values, such as $(0.7m_\rho, 0)$, $(m_\rho, 0)$, $(m_\rho, 3)$, $(m_\rho, 5)$, and $(3m_\rho, 5)$, the allowed parameter space which can give the correct size of the neutrino masses while satisfying flavor constraints are plotted as lines in the m_{H_2}-m_{A_0} plane in Fig. 3, which can be compared with the allowed parameter spaces (grey bands) from ΔT with the 1σ errors.

The general feature as seen from the diagrams in Fig. 3 is that with the relatively large couplings $\kappa_2 \gtrsim m_\rho$ and $\xi \gtrsim 3$, it is easy to obtain the correct neutrino masses while satisfying all constraints. And the final results are more sensitive to ξ than κ_2, since the integral $\mathcal{I}_2$ is generically larger than $\mathcal{I}_1$ with the chosen mass spectra. In particular, when $(\kappa_2, \xi) = (0.7m_\rho, 0)$ and $(m_\rho, 0)$, we cannot find any solution of (m_{H_2}, m_{A_0}) to realize enough neutrino masses in our phenomenologically interesting region, so we do not plot any lines for these two benchmarks in Fig. 3. Moreover, by comparing two diagrams in each line, the increase of m_ρ allows more parameter space in the m_{H_2}-m_{A_0} plane, while the careful examination of the three diagrams in either column shows that the parameter space shrinks when we enlarge m_{H_1}. The former phenomenon can be attributed to our assumption of $|C_{e\tau}| = 0.15(m_\rho/\mathrm{TeV})$ which effectively makes larger Yukawa couplings when amplifying m_ρ, while the latter can be understood as the decrease of the neutral scalar mass difference when m_{H_1} increases.

VIII. CONCLUSIONS

We have explored the cocktail model introduced in Ref. [10], which is interesting because it provides a connection between the origin of the small neutrino masses and the dark matter physics. In particular, we have shown the detailed derivation of the neutrino mass formulas in Eq. (4) from the three-loop cocktail diagrams, for which the subsequent loop integrals are calculated with the reliable numerical methods. Based on Eq. (4), the neutrino mass matrix is naturally predicted to be of the normal hierarchy type, with the nearly vanishing elements $(m_\nu)_{ee,e\mu}$. Consequently, the current data on the neutrino mass differences and mixings already fix the mass matrix to a high precision. By further considering the stringent constraints from the neutrinoless double beta decay, the low-energy LFV processes, the EWPT measurement of the T parameter, the DM relic density, and the collider searches, the DM mass is confined in the narrow range 60 GeV $< m_{H_0} <$ 75 GeV, and the right order of the neutrino masses can only be obtained by the large mass splittings for the neutral and charged scalars as well as the large couplings of $\kappa_2 \sim m_\rho$ and $\xi \gtrsim 3$. It is interesting to point out that the $0\nu\beta\beta$ decay is predominantly via the new short-distance contribution, which is typically larger than the usual long-distance one and has the possibility to be observed in the next-generation experiments.

ACKNOWLEDGMENTS

The work was supported in part by National Center for Theoretical Sciences, National Science Council (Grant No. NSC-101-2112-M-007-006-MY3) and National Tsing Hua University (Grant No. 103N2724E1).

APPENDIX: DETAILED CALCULATIONS OF THE COCKTAIL DIAGRAMS

In this appendix we compute the cocktail diagrams in the unitary gauge. Without loss of generality, we separate the neutrino mass into two parts, one proportional to κ_2 and the other ξv, which will be calculated in the following two subsections. In our numerical calculation, we study both zero and nonzero cases for ξ.

1. Integrals proportional to κ_2

In the unitary gauge, there are only eight Feynman diagrams in Fig. 1. Let us first focus on the upper triangle loops in the top of the diagrams, which are the only differences among the diagrams. The relevant pieces of the Lagrangian are

$$\begin{aligned}\mathcal{L} &= -\frac{ig_2}{\sqrt{2}}\Lambda^- W^{+\mu}\partial_\mu \Phi^0 - \kappa_2 \rho^{++} S^- S^- + \mathrm{H.c.}\\ &= -\frac{ig_2}{2}(c_\beta H_1^- - s_\beta H_2^-)W^{+\mu}\partial_\mu (H_0 + iA_0)\\ &\quad - \kappa_2 \rho^{++}(s_\beta^2 H_1^- H_1^- + 2c_\beta s_\beta H_1^- H_2^- + c_\beta^2 H_2^- H_2^-) + \mathrm{H.c.},\end{aligned} \tag{A1}$$

where $\Lambda^+ = c_\beta H_1^+ - s_\beta H_2^+$ and $S^+ = s_\beta H_1^+ + c_\beta H_2^+$. We choose $\langle H\rangle = (0, v)^T$ with $v = 173$ GeV. Using the Feynman rules, the triangle-loop factors involving H_0 are

$$\begin{aligned}&(H_0 H_1 H_1):\ (\kappa_2)\frac{g_2^2 s_{2\beta}^2}{8}\frac{(2k-k_2)_\nu(-2k-k_1)_\mu}{(k^2-m_{H_0}^2)[(k+k_1)^2-m_{H_1}^2][(k-k_2)^2-m_{H_1}^2]},\\ &(H_0 H_1 H_2):\ -(\kappa_2)\frac{g_2^2 s_{2\beta}^2}{8}\frac{(2k-k_2)_\nu(-2k-k_1)_\mu}{(k^2-m_{H_0}^2)[(k+k_1)^2-m_{H_1}^2][(k-k_2)^2-m_{H_2}^2]},\\ &(H_0 H_2 H_1):\ -(\kappa_2)\frac{g_2^2 s_{2\beta}^2}{8}\frac{(2k-k_2)_\nu(-2k-k_1)_\mu}{(k^2-m_{H_0}^2)[(k+k_1)^2-m_{H_2}^2][(k-k_2)^2-m_{H_1}^2]},\\ &(H_0 H_2 H_2):\ (\kappa_2)\frac{g_2^2 s_{2\beta}^2}{8}\frac{(2k-k_2)_\nu(-2k-k_1)_\mu}{(k^2-m_{H_0}^2)[(k+k_1)^2-m_{H_2}^2][(k-k_2)^2-m_{H_2}^2]},\end{aligned} \tag{A2}$$

while the corresponding factors for the diagrams involving the pseudoscalar A_0 are essentially the same with an additional minus sign. Thus, by summing these eight diagrams, we obtain

$$(\kappa_2)\frac{g_2^2 s_{2\beta}^2}{8}\int\frac{d^4k}{(2\pi)^4}\{(2k-k_2)_\nu(-2k-k_1)_\mu(\Delta m_+^2)^2\Delta m_0^2\}/\{(k^2-m_{H_0}^2)(k^2-m_{A_0}^2)$$
$$\times[(k+k_1)^2-m_{H_1}^2][(k+k_1)^2-m_{H_2}^2][(k-k_2)^2-m_{H_1}^2][(k-k_2)^2-m_{H_2}^2]\}, \tag{A3}$$

where $\Delta m_+^2 = m_{H_1}^2 - m_{H_2}^2$ and $\Delta m_0^2 = m_{H_0}^2 - m_{A_0}^2$. Note that the summation of all these diagrams effectively makes the integral in Eq. (A3) finite. By multiplying various common factors (propagators and vertices) in the cocktail diagrams, we get

$$(-im_\nu)_{ab} = \frac{s_{2\beta}}{(16\pi^2)^3}(x_a C_{ab} x_b)\left(\kappa_2 s_{2\beta}\frac{(\Delta m_+^2)^2\Delta m_0^2}{m_\rho^4 v^2}\right)$$
$$\times\frac{1}{2}(16\pi^2)^3 m_\rho^4 m_W^4 \gamma_\beta\gamma_\alpha\int\frac{d^4k_2}{(2\pi)^4}\int\frac{d^4k_1}{(2\pi)^4}\left\{\left(g^{\alpha\mu}-\frac{k_1^\alpha k_1^\mu}{m_W^2}\right)\left(g^{\beta\nu}-\frac{k_2^\beta k_2^\nu}{m_W^2}\right)\right\}\Big/$$
$$\{(k_2^2-m_W^2)(k_1^2-m_W^2)(k_2^2-m_a^2)(k_1^2-m_b^2)[(k_1+k_2)^2-m_\rho^2]\}$$
$$\times\int\frac{d^4k}{(2\pi)^4}\{(2k-k_2)_\nu(-2k-k_1)_\mu\}/\{(k^2-m_{H_0}^2)(k^2-m_{A_0}^2)[(k+k_1)^2-m_{H_1}^2]$$
$$\times[(k+k_1)^2-m_{H_2}^2][(k-k_2)^2-m_{H_1}^2][(k-k_2)^2-m_{H_2}^2]\}$$
$$= (x_a C_{ab} x_b)\frac{s_{2\beta}}{(16\pi^2)^3}\mathcal{A}_{1\kappa_2}\mathcal{I}_1, \tag{A4}$$

where we have used $x_a = m_a/v$ and $m_W = g_2 v/\sqrt{2}$ and rearranged the factors for convenience. Note that the prefactor $\mathcal{A}_{1\kappa_2}$ in the big parentheses is precisely the first part of $\mathcal{A}_1$ in Eq. (4) and we denote $\mathcal{I}_1$ for the three-loop integral shown in the last four lines of the first equality.

a. Integration over k

We now integrate the internal momentum k in Eq. (A4). By using the Feynman parameters s_i to combine the three pairs of the propagators with the same momentum, we have

$$\mathrm{I}_1 = \int\frac{d^4k}{(2\pi)^4}\{(2k-k_2)_\nu(-2k-k_1)_\mu\}/\{(k^2-m_{H_0}^2)(k^2-m_{A_0}^2)$$
$$\times[(k+k_1)^2-m_{H_1}^2][(k+k_1)^2-m_{H_2}^2][(k-k_2)^2-m_{H_1}^2][(k-k_2)^2-m_{H_2}^2]\}$$
$$= \int_0^1\prod_{i=1}^3 ds_i\int\frac{d^4k}{(2\pi)^4}\frac{(2k-k_2)_\nu(-2k-k_1)_\mu}{(k^2-m_{s_3}^2)^2[(k+k_1)^2-m_{s_1}^2]^2[(k-k_2)^2-m_{s_2}^2]^2}, \tag{A5}$$

where we have defined $m_{s_1}^2 = (1-s_1)m_{H_1}^2 + s_1 m_{H_2}^2$, $m_{s_2}^2 = (1-s_2)m_{H_1}^2 + s_2 m_{H_2}^2$, and $m_{s_3}^2 = (1-s_3)m_{H_0}^2 + s_3 m_{A_0}^2$. The combination of the remaining three factors in the denominator above gives

$$\mathrm{I}_1 = \int_0^1\prod_{i=1}^3 ds_i\Gamma(6)\int dx_1 dx_2\int\frac{d^4k}{(2\pi)^4}\{x_1x_2(1-x_1-x_2)(2k-k_2)_\nu(-2k-k_1)_\mu\}/$$
$$(x_1[(k+k_1)^2-m_{s_1}^2]+x_2[(k-k_2)^2-m_{s_2}^2]+(1-x_1-x_2)[k^2-m_{s_3}^2])^6$$
$$= \int_0^1\prod_{i=1}^3 ds_i\Gamma(6)\int dx_1dx_2x_1x_2(1-x_1-x_2)\int\frac{d^4k}{(2\pi)^4}\frac{-4k_\mu k_\nu+[-(1-2x_1)k_1-2x_2k_2]_\mu[-2x_1k_1+(2x_2-1)k_2]_\nu}{(k^2-m_x^2)^6}, \tag{A6}$$

where we have made the translation of the momentum $k\to k-x_1k_1+x_2k_2$ and defined

$$m_x^2 = \sum_i^{i=3} x_i m_{s_i}^2 - x_1(1-x_1)k_1^2 - 2x_1x_2k_1\cdot k_2 - x_2(1-x_2)k_2^2, \tag{A7}$$

with $x_3 = 1 - x_1 - x_2$. We have also ignored the terms proportional to the odd powers of k since they vanish after the integration. The integration over k leads to

$$\mathrm{I}_1 = \int_0^1 \prod_{i=1}^{3} ds_i \int dx_1 dx_2 x_1 x_2 (1 - x_1 - x_2) \frac{i}{16\pi^2} \Gamma(3) \times \left(\frac{2 g_{\mu\nu}}{(m_x^2)^3} + \frac{3 N_{\mu\nu}}{(m_x^2)^4} \right), = \mathrm{I}_{11} + \mathrm{I}_{12}, \tag{A8}$$

where

$$N_{\mu\nu} = [-(1 - 2x_1)k_1 - 2x_2 k_2]_\mu [-2x_1 k_1 + (2x_2 - 1)k_2]_\nu. \tag{A9}$$

b. Integration of I_{11} over k_1 and k_2

The integration over k_1 for I_{11} is defined as

$$\mathrm{II}_1 = \frac{i}{16\pi^2} \Gamma(3) x_1 x_2 (1 - x_1 - x_2) \int \frac{d^4 k_1}{(2\pi)^4} \times \frac{[g^{\alpha\mu} - k_1^\alpha k_1^\mu / m_W^2]}{(k_1^2 - m_W^2)(k_1^2 - m_b^2)[(k_1 + k_2)^2 - m_\rho^2]} \frac{2 g_{\mu\nu}}{(m_x^2)^3}, \tag{A10}$$

where we have suppressed the integration measure for the Feynman parameters x_j and s_i to simplify our formulas. With the Feynman parameters z_i $(i = 1, \ldots 3)$, we can combine all the factors in the denominator

$$\mathrm{II}_1 = \frac{i\Gamma(3)}{16\pi^2} \frac{(-1) x_1 x_2 (1 - x_1 - x_2)}{x_1^3 (1 - x_1)^3} \frac{\Gamma(6)}{\Gamma(3)} \times \int \prod_{j=3}^{3} dz_j \frac{2 z_1^2 [g_\nu^\alpha - k_1^\alpha k_{1\nu} / m_W^2]}{D^6}, \tag{A11}$$

where

$$D = z_1 \left[k_1^2 + \frac{2 x_1 x_2}{x_1 (1 - x_1)} k_1 \cdot k_2 + \frac{x_2 (1 - x_2)}{x_1 (1 - x_1)} k_2^2 - \frac{\sum_i x_i m_{s_i}^2}{x_1 (1 - x_1)} \right] + z_2 [(k_1 + k_2)^2 - m_\rho^2] + z_3 (k_1^2 - m_W^2) + (1 - z_1 - z_2 - z_3)(k_1^2 - m_b^2). \tag{A12}$$

With the internal momentum translation $k_1 \to k_1 - c_2 k_2$, where $c_2 = [x_2 z_1 + (1 - x_1) z_2]/(1 - x_1)$, and the integration of k_1, we obtain

$$\mathrm{II}_1 = \frac{1}{(16\pi^2)^2} \int \prod_{j=1}^{3} dz_j \frac{x_1 x_2 (1 - x_1 - x_2) z_1^2}{x_1^3 (1 - x_1)^3} \times \left\{ \frac{2\Gamma(4)(g_\nu^\alpha - c_2^2 k_2^\alpha k_{2\nu} / m_W^2)}{B_2^4 [k_2^2 - \Delta]^4} - \frac{\Gamma(3)}{m_W^2} \frac{g_\nu^\alpha}{B_2^3 [k_2^2 - \Delta]^3} \right\}, \tag{A13}$$

where

$$B_2 = \frac{x_2 (1 - x_2) z_1}{x_1 (1 - x_1)} + z_2 - c_2^2, \tag{A14}$$

$$\Delta = \frac{z_2}{B_2} m_\rho^2 + \frac{z_3}{B_2} m_W^2 + \frac{1 - z_1 - z_2 - z_3}{B_2} m_b^2 + \frac{z_1 \sum_i x_i m_{s_i}^2}{B_2 x_1 (1 - x_1)}. \tag{A15}$$

The integration over k_2 can be similarly done and the result is given by

$$\mathrm{III}_1 = \frac{\Gamma(3)}{(16\pi^2)^2} \frac{x_1 x_2 (1 - x_1 - x_2) z_1^2}{x_1^3 (1 - x_1)^3} \times \int \frac{d^4 k_2}{(2\pi)^4} \frac{(g^{\beta\nu} - k_2^\beta k_2^\nu / m_W^2)}{(k_2^2 - m_W^2)(k_2^2 - m_a^2)} \times \left\{ \frac{6(g_\nu^\alpha - c_2^2 k_2^\alpha k_{2\nu} / m_W^2)}{B_2^4 [k_2^2 - \Delta]^4} - \frac{1}{m_W^2} \frac{g_\nu^\alpha}{B_2^3 [k_2^2 - \Delta]^3} \right\}, \tag{A16}$$

where the integration measures for the Feynman parameters are also suppressed for simplicity. By combining the factors in the denominator with the Feynman parameters y_i, the expression can be transformed into

$$\mathrm{III}_1 = \frac{\Gamma(3)}{(16\pi^2)^2} \frac{x_1 x_2 (1 - x_1 - x_2) z_1^2}{x_1^3 (1 - x_1)^3} \int dy_1 dy_2 \times \int \frac{d^4 k_2}{(2\pi)^4} (g^{\beta\nu} - k_2^\beta k_2^\nu / m_W^2) \times \left\{ \frac{\Gamma(6)}{\Gamma(4)} \frac{6 y_1^3}{B_2^4} \frac{(g_\nu^\alpha - c_2^2 k_2^\alpha k_{2\nu} / m_W^2)}{(k_2^2 - [m_\rho^2 \Sigma]/[B_2 x_1 (1 - x_1)])^6} - \frac{\Gamma(5)}{\Gamma(3)} \frac{y_1^2}{m_W^2 B_2^3} \frac{g_\nu^\alpha}{(k_2^2 - [m_\rho^2 \Sigma]/[B_2 x_1 (1 - x_1)])^5} \right\}, \tag{A17}$$

where

$$\Sigma = x_1 (1 - x_1) \left[y_1 z_2 + (y_1 z_3 + y_2 B_2) \frac{m_W^2}{m_\rho^2} + y_1 (1 - z_1 - z_2 - z_3) \frac{m_b^2}{m_\rho^2} + (1 - y_1 - y_2) B_2 \frac{m_a^2}{m_\rho^2} \right] + y_1 z_1 \frac{(\sum_i x_i m_{s_i}^2)}{m_\rho^2}. \tag{A18}$$

After integrating out k_2, we find

$$\mathrm{III}_1 = \frac{i}{(16\pi^2)^3}[x_1x_2(1-x_1-x_2)z_1^2]\frac{g^{\alpha\beta}}{4}\left\{y_1^3\left[\frac{48x_1(1-x_1)}{m_\rho^8\Sigma^4}+\frac{8(c_2^2+1)}{m_W^2m_\rho^6B_2\Sigma^3}+\frac{12c_2^2}{m_W^4m_\rho^4B_2^2x_1(1-x_1)\Sigma^2}\right]\right.$$
$$\left.+y_1^2\left[\frac{8}{m_W^2m_\rho^6\Sigma^3}+\frac{2}{m_W^4m_\rho^4B_2x_1(1-x_1)\Sigma^2}\right]\right\}. \tag{A19}$$

c. Integration of I_{12} *over* k_1 *and* k_2

The integration over k_1 for I_{12} can be written as

$$\mathrm{II}_2 = \frac{i}{16\pi^2}\Gamma(3)x_1x_2(1-x_1-x_2)\int\frac{d^4k_1}{(2\pi)^4}\frac{(g^{\alpha\mu}-k_1^\alpha k_1^\mu/m_W^2)}{(k_1^2-m_W^2)(k_1^2-m_b^2)[(k_1+k_2)^2-m_\rho^2]}\frac{3N_{\mu\nu}}{(m_x^2)^4}, \tag{A20}$$

where we have also suppressed the Feynman parameter integration measures. Similar to the derivation of Eq. (A11) from Eq. (A10), we have

$$\mathrm{II}_2 = \frac{i}{16\pi^2}\frac{x_1x_2(1-x_1-x_2)}{x_1^4(1-x_1)^4}\Gamma(7)z_1^3\int\frac{d^4k_1}{(2\pi)^4}\frac{N_\nu^{\prime\alpha}}{D^7}, \tag{A21}$$

where D is defined in Eq. (A12) and

$$\begin{aligned}
N_\nu^{\prime\alpha} &= [-(1-2x_1)(k_1-c_2k_2)-2x_2k_2]_\mu[-2x_1(k_1-c_2k_2)+(2x_2-1)k_2]_\nu[g^{\alpha\mu}-(k_1-ck_2)^\alpha(k_1-c_2k_2)^\mu/m_W^2]\\
&= (1-2x_1)(2x_1)k_1^\alpha k_{1\nu}+d_1d_2k_2^\alpha k_{2\nu}-(1-2x_1)(2x_1)\frac{1}{m_W^2}k_1^2k_1^\alpha k_{1\nu}\\
&\quad -(1-2x_1)(2x_1)c_2^2\frac{1}{m_W^2}k_1\cdot k_2k_2^\alpha k_{1\nu}-(1-2x_1)d_2c_2\frac{1}{m_W^2}k_1\cdot k_2k_1^\alpha k_{2\nu}\\
&\quad -(1-2x_1)d_2c_2\frac{1}{m_W^2}k_1^2k_2^\alpha k_{2\nu}-(2x_1)d_1c_2\frac{1}{m_W^2}k_2^2k_1^\alpha k_{1\nu}\\
&\quad -(2x_1)d_1c_2\frac{1}{m_W^2}k_1\cdot k_2k_2^\alpha k_{1\nu}-d_1d_2\frac{1}{m_W^2}k_1\cdot k_2k_1^\alpha k_{2\nu}-d_1d_2c_2^2\frac{1}{m_W^2}k_2^2k_2^\alpha k_{2\nu},
\end{aligned} \tag{A22}$$

with

$$d_1 = c_2-2c_2x_1-2x_2, \qquad d_2 = 2x_1c_2+2x_2-1. \tag{A23}$$

The integration over k_1 can be easily carried out with the result given by

$$\begin{aligned}
\mathrm{II}_2 = \frac{\Gamma(3)}{(16\pi^2)^2}\frac{x_1x_2(1-x_1x_2)z_1^3}{x_1^4(1-x_1)^4}&\left\{-\frac{12d_1d_2k_2^\alpha k_{2\nu}}{B_2^5[k_2^2-\Delta]^5}+\frac{12d_1d_2c_2^2k_2^2k_2^\alpha k_{2\nu}}{B_2^5m_W^2[k_2^2-\Delta]^5}-\frac{6(1-2x_1)(2x_1)g_\nu^\alpha}{4B_2^4[k_2^2-\Delta]^4}\right.\\
&+\frac{6(1-2x_1)(2x_1)c_2^2k_{2\nu}k_2^\alpha}{4B_2^4m_W^2[k_2^2-\Delta]^4}+\frac{6(1-2x_1)d_2c_2k_{2\nu}k_2^\alpha}{4B_2^4m_W^2[k_2^2-\Delta]^4}+\frac{6(1-2x_1)d_2c_2k_{2\nu}k_2^\alpha}{B_2^4m_W^2[k_2^2-\Delta]^4}\\
&\left.+\frac{6(2x_1)d_1c_2g_\nu^\alpha k_2^2}{4B_2^4m_W^2[k_2^2-\Delta]^4}+\frac{6(2x_1)d_1c_2k_{2\nu}k_2^\alpha}{4B_2^4m_W^2[k_2^2-\Delta]^4}+\frac{6d_1d_2k_{2\nu}k_2^\alpha}{4B_2^4m_W^2[k_2^2-\Delta]^4}+\frac{6(1-2x_1)(2x_1)g_\nu^\alpha}{4B_2^3m_W^2[k_2^2-\Delta]^3}\right\}.
\end{aligned} \tag{A24}$$

By appending the rest propagators involving k_2 and performing the Feynman parametrization with y_i as that in Eq. (A17), the expression becomes

$$\begin{aligned}
\mathrm{III}_2 &= \int \frac{d^4k_2}{(2\pi)^4} \frac{\left(g^{\beta\nu} - \frac{k_2^\beta k_2^\nu}{m_W^2}\right)}{(k_2^2 - m_W^2)(k_2^2 - m_a^2)} \mathrm{II}_2 \\
&= \frac{1}{(16\pi^2)^2} \frac{x_1 x_2 (1 - x_1 - x_2) z_1^3}{x_1^4 (1 - x_1)^4} \int \frac{d^4k_2}{(2\pi)^4} \left\{ -\frac{\Gamma(7) d_1 d_2 y_1^4}{B_2^5} \frac{k_2^\alpha k_2^\beta \left(1 - \frac{k_2^2}{m_W^2}\right)}{[k_2^2 - (m_\rho^2 \Sigma)/(x_1(1 - x_1)B_2)]^7} \right. \\
&\quad + \frac{\Gamma(7) d_1 d_2 c_2^2 y_1^4}{B_2^5} \frac{k_2^\alpha k_2^\beta k_2^2 \left(1 - \frac{k_2^2}{m_W^2}\right)}{m_W^2 [k_2^2 - (m_\rho^2 \Sigma)/(x_1(1 - x_1)B_2)]^7} - \frac{\Gamma(6)(1 - 2x_1)(2x_1) y_1^3}{2B_2^4} \frac{\left(g^{\alpha\beta} - \frac{k_2^\alpha k_2^\beta}{m_W^2}\right)}{[k_2^2 - (m_\rho^2 \Sigma)/(x_1(1 - x_1)B_2)]^6} \\
&\quad + \frac{\Gamma(6)(1 - 2x_1)(2x_1) c_2^2 y_1^3}{2B_2^4} \frac{k_2^\alpha k_2^\beta \left(1 - \frac{k_2^2}{m_W^2}\right)}{m_W^2 [k_2^2 - (m_\rho^2 \Sigma)/(x_1(1 - x_1)B_2)]^6} \\
&\quad + \frac{\Gamma(6)(1 - 2x_1) d_2 c_2 y_1^3}{2B_2^4} \frac{k_2^\alpha k_2^\beta \left(1 - \frac{k_2^2}{m_W^2}\right)}{m_W^2 [k_2^2 - (m_\rho^2 \Sigma)/(x_1(1 - x_1)B_2)]^6} + \frac{2\Gamma(6)(1 - 2x_1) d_2 c_2 y_1^3}{B_2^4} \frac{k_2^\alpha k_2^\beta \left(1 - \frac{k_2^2}{m_W^2}\right)}{m_W^2 [k_2^2 - (m_\rho^2 \Sigma)/(x_1(1 - x_1)B_2)]^6} \\
&\quad + \frac{\Gamma(6)(2x_1) d_1 c_2 y_1^3}{2B_2^4} \frac{k_2^2 \left(g^{\alpha\beta} - \frac{k_2^\alpha k_2^\beta}{m_W^2}\right)}{m_W^2 [k_2^2 - (m_\rho^2 \Sigma)/(x_1(1 - x_1)B_2)]^6} + \frac{\Gamma(6)(2x_1) d_1 c_2 y_1^3}{2B_2^4} \frac{k_2^\alpha k_2^\beta \left(g^{\alpha\beta} - \frac{k_2^2}{m_W^2}\right)}{m_W^2 [k_2^2 - (m_\rho^2 \Sigma)/(x_1(1 - x_1)B_2)]^6} \\
&\quad \left. + \frac{\Gamma(6) d_1 d_2 y_1^3}{2B_2^4} \frac{k_2^\alpha k_2^\beta \left(1 - \frac{k_2^2}{m_W^2}\right)}{m_W^2 [k_2^2 - (m_\rho^2 \Sigma)/(x_1(1 - x_1)B_2)]^6} + \frac{6\Gamma(5)(1 - 2x_1)(2x_1) y_1^2}{4B_2^3} \frac{g^{\alpha\beta} - \frac{k_2^\alpha k_2^\beta}{m_W^2}}{m_W^2 [k_2^2 - (m_\rho^2 \Sigma)/(x_1(1 - x_1)B_2)]^5} \right\}.
\end{aligned} \tag{A25}$$

Finally, the integration over k_2 gives

$$\begin{aligned}
\mathrm{III}_2 = \frac{i}{(16\pi^2)^3} x_1 x_2 (1 - x_1 - x_2) z_1^3 \frac{g^{\alpha\beta}}{4} &\left\{ -d_1 d_2 y_1^4 \left(\frac{12}{B_2 \Sigma^4 m_\rho^8} + \frac{12}{x_1(1 - x_1) B_2^2 \Sigma^3 m_\rho^6 m_W^2} \right) \right. \\
&- d_1 d_2 c_2^2 y_1^4 \left(\frac{12}{x_1(1 - x_1) B_2^2 \Sigma^3 m_\rho^6 m_W^2} + \frac{24}{x_1^2 (1 - x_1)^2 B_2^3 \Sigma^2 m_\rho^4 m_W^4} \right) \\
&- 2x_1 (1 - 2x_1) y_1^3 \left(\frac{12}{\Sigma^4 m_\rho^8} + \frac{2}{x_1(1 - x_1) B_2 \Sigma^3 m_\rho^6 m_W^2} \right) \\
&- 2x_1 (1 - 2x_1) c_2^2 y_1^3 \left(\frac{2}{x_1(1 - x_1) B_2 \Sigma^3 m_\rho^6 m_W^2} + \frac{3}{x_1^2 (1 - x_1)^2 B_2^2 \Sigma^2 m_\rho^4 m_W^4} \right) \\
&- (1 - 2x_1) d_2 c_2 y_1^3 \left(\frac{2}{x_1(1 - x_1) B_2 \Sigma^3 m_\rho^6 m_W^2} + \frac{3}{x_1^2 (1 - x_1)^2 B_2^2 \Sigma^2 m_\rho^4 m_W^4} \right) \\
&- (1 - 2x_1) d_2 c_2 y_1^3 \left(\frac{8}{x_1(1 - x_1) B_2 \Sigma^3 m_\rho^6 m_W^2} + \frac{12}{x_1^2 (1 - x_1)^2 B_2^2 \Sigma^2 m_\rho^4 m_W^4} \right) \\
&- 2x_1 d_1 c_2 y_1^3 \left(\frac{8}{x_1(1 - x_1) B_2 \Sigma^3 m_\rho^6 m_W^2} + \frac{3}{x_1^2 (1 - x_1)^2 B_2^2 \Sigma^2 m_\rho^4 m_W^4} \right) \\
&- 2x_1 d_1 c_2 y_1^3 \left(\frac{2}{x_1(1 - x_1) B_2 \Sigma^3 m_\rho^6 m_W^2} + \frac{3}{x_1^2 (1 - x_1)^2 B_2^2 \Sigma^2 m_\rho^4 m_W^4} \right) \\
&- d_1 d_2 y_1^3 \left(\frac{2}{x_1(1 - x_1) B_2 \Sigma^3 m_\rho^6 m_W^2} + \frac{3}{x_1^2 (1 - x_1)^2 B_2^2 \Sigma^2 m_\rho^4 m_W^4} \right) \\
&\left. - (1 - 2x_1)(2x_1) y_1^2 \left(\frac{12}{x_1(1 - x_1) \Sigma^3 m_\rho^6 m_W^2} + \frac{3}{x_1^2 (1 - x_1)^2 B_2 \Sigma^2 m_\rho^4 m_W^4} \right) \right\}.
\end{aligned} \tag{A26}$$

d. Final results

By summing up the above two integration results and multiplying the prefactors, we obtain

$$\mathcal{I}_1 = \frac{1}{2}(16\pi^2)^3 m_\rho^4 m_W^4 \gamma_\beta \gamma_\alpha (\mathrm{III}_1 + \mathrm{III}_2) = \frac{i}{2}\left(\frac{m_W^4}{m_\rho^4}\mathcal{I}_{12} + \frac{m_W^2}{m_\rho^2}\mathcal{I}_{11} + \mathcal{I}_{10}\right), \tag{A27}$$

with

$$\mathcal{I}_{10} = \frac{x_1 x_2 (1 - x_1 - x_2) z_1^2}{\Sigma^4}\left(48 x_1 (1 - x_1) y_1^3 - \frac{12 d_1 d_2 y_1^4 z_1}{B_2} - 12(1 - 2x_1)(2x_1) y_1^3 z_1\right), \tag{A28}$$

$$\begin{aligned}\mathcal{I}_{11} = {} & \frac{x_1 x_2 (1 - x_1 - x_2) z_1^2}{\Sigma^3}\left(\frac{8 y_1^3 (c_2^2 + 1)}{B_2} + 8 y_1^2\right) + \frac{x_1 x_2 (1 - x_1 - x_2) z_1^3}{x_1 (1 - x_1) \Sigma^3}\left(-\frac{12 d_1 d_2 y_1^4}{B_2^2}\right. \\ & - \frac{12 d_1 d_2 c_2^2 y_1^4}{B_2^2} - \frac{2(1 - 2x_1)(2x_1) y_1^3}{B_2} - \frac{2(1 - 2x_1)(2x_1) c_2^2 y_1^3}{B_2} - \frac{2(1 - 2x_1) d_2 c_2 y_1^3}{B_2} \\ & \left. - \frac{8(1 - 2x_1) d_2 c_2 y_1^3}{B_2} - \frac{8(2x_1) d_1 c_2 y_1^3}{B_2} - \frac{2(2x_1) d_1 c_2 y_1^3}{B_2} - \frac{2 d_1 d_2 y_1^3}{B_2} - 12(1 - 2x_1)(2x_1) y_1^2\right),\end{aligned} \tag{A29}$$

$$\begin{aligned}\mathcal{I}_{12} = {} & \frac{x_1 x_2 (1 - x_1 - x_2) z_1^2}{x_1 (1 - x_1) \Sigma^2}\left(\frac{12 y_1^3 c_2^2}{B_2^2} + \frac{2 y_1^2}{B_2}\right) + \frac{x_1 x_2 (1 - x_1 - x_2) z_1^3}{x_1^2 (1 - x_1)^2 \Sigma^2}\left(-\frac{24 d_1 d_2 c_2^2 y_1^4}{B_2^3}\right. \\ & - \frac{3(1 - 2x_1)(2x_1) c_2^2 y_1^3}{B_2^2} - \frac{3(1 - 2x_1) d_2 c_2 y_1^3}{B_2^2} - \frac{12(1 - 2x_1) d_2 c_2 y_1^3}{B_2^2} - \frac{3(2x_1) d_1 c_2 y_1^3}{B_2^2} \\ & \left. - \frac{3(2x_1) d_1 c_2 y_1^3}{B_2^2} - \frac{3 d_1 d_2 y_1^3}{B_2^2} - \frac{3(1 - 2x_1)(2x_1) y_1^2}{B_2}\right),\end{aligned} \tag{A30}$$

where the final results are classified according to the powers of m_W^2/m_ρ^2. Here, we have suppressed the integration measures for the Feynman parameters x_i, y_i, z_i, and s_i, defined by

$$\text{measure} = \int_0^1 ds_1 \int_0^1 ds_2 \int_0^1 ds_3 \int_0^1 dx_1 \int_0^{1-x_1} dx_2 \int_0^1 dy_1 \int_0^{1-y_1} dy_2 \int_0^1 dz_1 \int_0^{1-z_1} dz_2 \int_0^{1-z_1-z_2} dz_3. \tag{A31}$$

It is clear that this complicated 10-dimensional Feynman parameter integration can only be calculated with the help of a numerical package. In our work, we use three widely applied numerical integration applications: MATHEMATICA (Global Adaptive), SECDEC-2.1.4 [11] and VEGAS in GSL [12] in order to cross-check the accuracy and stability of the calculation. With Eq. (A27), we can study the benchmark point:

$$\begin{aligned} & m_{H^0} = 70\ \text{GeV}, \quad m_{A^0} = 250\ \text{GeV}, \quad m_{H_1^+} = 90\ \text{GeV}, \quad m_{H_2^+} = 400\ \text{GeV}, \quad m_\rho = 1\ \text{TeV}, \\ & C_{e\tau} = 0.06, \quad C_{\mu\mu} = 0.01, \quad C_{\mu\tau} = 0.0009, \quad C_{\tau\tau} = 5 \times 10^{-5}, \quad \kappa_2 = 2\ \text{TeV}\end{aligned} \tag{A32}$$

in the first version of Ref. [10] before its erratum with $\xi = 0$, and the final results are given by

$$\begin{aligned} \text{Mathematica:} \quad & \mathcal{I}_{10} = 7264.5 \pm 104.4, \quad \mathcal{I}_{11} = 124.667 \pm 1.818, \quad \mathcal{I}_{12} = 4.10278 \pm 0.0234; \\ & \mathcal{I}_1 = 2.61 i, \quad m_\nu = \begin{pmatrix} \mathcal{O}(10^{-3}) & \mathcal{O}(10^{-3}) & 1.05 \\ \mathcal{O}(10^{-3}) & 2.16 & 3.25 \\ 1.05 & 3.25 & 3.03 \end{pmatrix} \times 10^{-13}\ \text{GeV},\end{aligned} \tag{A33}$$

$$\text{GSL–VEGAS:}\quad \mathcal{I}_{10} = 7350.752 \pm 5.271, \quad \mathcal{I}_{11} = 125.122 \pm 0.116, \quad \mathcal{I}_{12} = 4.107 \pm 0.003;$$

$$\mathcal{I}_1 = 2.612i, \qquad m_\nu = \begin{pmatrix} \mathcal{O}(10^{-3}) & \mathcal{O}(10^{-3}) & 1.05 \\ \mathcal{O}(10^{-3}) & 2.16 & 3.26 \\ 1.05 & 3.26 & 3.04 \end{pmatrix} \times 10^{-13}\ \text{GeV}, \tag{A34}$$

$$\text{SecDec-2.1.4:}\quad \mathcal{I}_{10} = 7353.2 \pm 7.3, \quad \mathcal{I}_{11} = 125.79 \pm 0.04, \quad \mathcal{I}_{12} = 4.108 \pm 0.001;$$

$$\mathcal{I}_1 = 2.612i, \qquad m_\nu = \begin{pmatrix} \mathcal{O}(10^{-3}) & \mathcal{O}(10^{-3}) & 1.05 \\ \mathcal{O}(10^{-3}) & 2.16 & 3.26 \\ 1.05 & 3.26 & 3.04 \end{pmatrix} \times 10^{-13}\ \text{GeV}. \tag{A35}$$

As expected, the numerical values from the three packages are essentially the same. Clearly, the obtained neutrino masses with $\xi = 0$ are smaller than the experimental values by about 2 orders.

2. Integrals proportional to ξv

In this subsection, we go on to calculate the neutrino mass part which is proportional to ξv. The relevant pieces of the Lagrangian are

$$\begin{aligned} \mathcal{L}_\xi &= -\xi \Phi_2^T i\sigma_2 \Phi_1 S^+ \rho^{--} + \text{H.c.} = -\xi v \Lambda^+ S^+ \rho^{--} + \text{H.c.} \\ &= -\xi v \rho^{--} [s_\beta c_\beta H_1^+ H_1^+ + (c_\beta^2 - s_\beta^2) H_1^+ H_2^+ - s_\beta c_\beta H_2^+ H_2^+] + \text{H.c.} \end{aligned} \tag{A36}$$

These vertices, together with the first term in Eq. (A1), also give eight Feynman diagrams in the unitary gauge with the upper triangle loops as their only differences. Among them, the four triangle factors with H_0 running inside are

$$\begin{aligned} (H_0 H_1 H_1):&\ (\xi v) \frac{g_2^2 s_{2\beta}(c_{2\beta}+1)}{8} \frac{(2k-k_2)_\nu (-2k-k_1)_\mu}{(k^2 - m_{H_0}^2)[(k+k_1)^2 - m_{H_1}^2][(k-k_2)^2 - m_{H_1}^2]}, \\ (H_0 H_1 H_2):&\ -(\xi v) \frac{g_2^2 s_{2\beta} c_{2\beta}}{8} \frac{(2k-k_2)_\nu (-2k-k_1)_\mu}{(k^2 - m_{H_0}^2)[(k+k_1)^2 - m_{H_1}^2][(k-k_2)^2 - m_{H_2}^2]}, \\ (H_0 H_2 H_1):&\ -(\xi v) \frac{g_2^2 s_{2\beta} c_{2\beta}}{8} \frac{(2k-k_2)_\nu (-2k-k_1)_\mu}{(k^2 - m_{H_0}^2)[(k+k_1)^2 - m_{H_2}^2][(k-k_2)^2 - m_{H_1}^2]}, \\ (H_0 H_2 H_2):&\ (\xi v) \frac{g_2^2 s_{2\beta}(c_{2\beta}-1)}{8} \frac{(2k-k_2)_\nu (-2k-k_1)_\mu}{(k^2 - m_{H_0}^2)[(k+k_1)^2 - m_{H_2}^2][(k-k_2)^2 - m_{H_2}^2]}, \end{aligned} \tag{A37}$$

while an extra overall minus sign should be multiplied for the corresponding formulas involving the pseudoscalar A_0. Thus, the summation of all eight diagrams yields

$$\begin{aligned} &(\xi v) \frac{g_2^2 s_{2\beta} c_{2\beta}}{8} \int \frac{d^4 k}{(2\pi)^4} \{(2k-k_2)_\nu (-2k-k_1)_\mu (\Delta m_+^2)^2 \Delta m_0^2\} / \{(k^2 - m_{H_0}^2)(k^2 - m_{A_0}^2)[(k+k_1)^2 - m_{H_1}^2] \\ &\quad \times [(k+k_1)^2 - m_{H_2}^2][(k-k_2)^2 - m_{H_1}^2][(k-k_2)^2 - m_{H_2}^2]\} \\ &\quad + (\xi v) \frac{g_2^2 s_{2\beta}}{8} \int \frac{d^4 k}{(2\pi)^4} \left\{ \frac{(2k-k_2)_\nu (-2k-k_1)_\mu \Delta m_+^2 \Delta m_0^2}{(k^2 - m_{H_0}^2)(k^2 - m_{A_0}^2)[(k+k_1)^2 - m_{H_1}^2][(k-k_2)^2 - m_{H_1}^2][(k-k_2)^2 - m_{H_2}^2]} \right. \\ &\quad \left. + \frac{(2k-k_2)_\nu (-2k-k_1)_\mu \Delta m_+^2 \Delta m_0^2}{(k^2 - m_{H_0}^2)(k^2 - m_{A_0}^2)[(k+k_1)^2 - m_{H_1}^2][(k+k_1)^2 - m_{H_2}^2][(k-k_2)^2 - m_{H_2}^2]} \right\}. \end{aligned} \tag{A38}$$

Note that the integral in the first two lines is the same as that proportional to κ_2 in Eq. (A3), so we expect that it gives the same result $\mathcal{I}_1$. Thus, the contribution to neutrino masses proportional to ξ can be written as

$$(-im_\nu)_{ab} = (x_a C_{ab} x_b)\frac{s_{2\beta}}{(16\pi^2)^3}(\mathcal{A}_{1\xi}\mathcal{I}_1 + \mathcal{A}_2\mathcal{I}_2), \tag{A39}$$

where

$$\mathcal{A}_{1\xi} = \xi v c_{2\beta}\frac{(\Delta m_+^2)^2 \Delta m_0^2}{m_\rho^4 v^2}, \qquad \mathcal{A}_2 = \frac{\xi v}{m_\rho^2}\frac{\Delta m_+^2 \Delta m_0^2}{v^2} \tag{A40}$$

$$\begin{aligned}\mathcal{I}_2 &= \frac{1}{2}(16\pi^2)^3 m_\rho^2 m_W^4 \gamma_\beta \gamma_\alpha \int \frac{d^4k_2}{(2\pi)^4}\int \frac{d^4k_1}{(2\pi)^4}\frac{(g^{\alpha\mu} - \frac{k_1^\alpha k_1^\mu}{m_W^2})(g^{\beta\nu} - \frac{k_2^\beta k_2^\nu}{m_W^2})}{(k_2^2 - m_W^2)(k_1^2 - m_W^2)(k_2^2 - m_a^2)(k_1^2 - m_b^2)[(k_1+k_2)^2 - m_\rho^2]} \\ &\quad \times \int \frac{d^4k}{(2\pi)^4}\left\{\frac{(2k-k_2)_\nu(-2k-k_1)_\mu}{(k^2 - m_{H_0}^2)(k^2 - m_{A_0}^2)[(k+k_1)^2 - m_{H_1}^2][(k-k_2)^2 - m_{H_1}^2][(k-k_2)^2 - m_{H_2}^2]}\right. \\ &\quad \left. + \frac{(2k-k_2)_\nu(-2k-k_1)_\mu}{(k^2 - m_{H_0}^2)(k^2 - m_{A_0}^2)[(k+k_1)^2 - m_{H_1}^2][(k+k_1)^2 - m_{H_2}^2][(k-k_2)^2 - m_{H_2}^2]}\right\} \\ &= \mathcal{I}_2' + \mathcal{I}_2''. \end{aligned} \tag{A41}$$

Here, we have separated $\mathcal{I}_2$ into two parts, $\mathcal{I}_2'$ and $\mathcal{I}_2''$, which are defined in the second and third lines in the first equality, respectively. Note that $\mathcal{I}_2'$ and $\mathcal{I}_2''$ are symmetric to each other by the exchange of the charged scalar masses $m_{H_1}^2 \leftrightarrow m_{H_2}^2$. Thus, in practice, we only need to calculate $\mathcal{I}_2'$ and find the result of $\mathcal{I}_2''$ with such a mass exchange, as is done in the following subsections.

a. Integration over k

We first integrate k in $\mathcal{I}_2'$. With the Feynman parameters s_i and x_i, we combine the propagators in the denominator as follows:

$$\mathrm{I}_1' = \int_0^1 \prod_{i=1}^3 ds_i \Gamma(5)\int dx_1 dx_2 x_2(1-x_1-x_2)\int \frac{d^4k}{(2\pi)^4}\frac{-4k_\mu k_\nu + [-(1-2x_1)k_1 - 2x_2k_2]_\mu[-2x_1k_1 + (2x_2-1)k_2]_\nu}{(k^2 - m_x'^2)^5}, \tag{A42}$$

where we have made the translation of the momentum $k \to k - x_1k_1 + x_2k_2$ and defined

$$m_x'^2 = m_\sigma^2 - x_1(1-x_1)k_1^2 - 2x_1x_2k_1\cdot k_2 - x_2(1-x_2)k_2^2, \tag{A43}$$

with $m_\sigma^2 \equiv x_1 m_{H_1}^2 + \sum_{i=2}^3 x_i m_{s_i}^2$ and $x_3 = 1 - x_1 - x_2$. The integration over k can be subsequently performed with the following results:

$$\begin{aligned}\mathrm{I}_1' &= \int_0^1 \prod_{i=2}^3 ds_i \int dx_1 dx_2 x_2(1-x_1-x_2)\frac{(-i)}{16\pi^2} \\ &\quad \times \left[\frac{2g_{\mu\nu}}{(m_x'^2)^2} + \frac{2N_{\mu\nu}}{(m_x'^2)^3}\right] \\ &= \mathrm{I}_{11}' + \mathrm{II}_{12}',\end{aligned} \tag{A44}$$

where $N_{\mu\nu}$ is the same as in Eq. (A9). We have separated I_1' into II_{11}' and I_{12}' in terms of their powers of $m_x'^2$.

b. Integration of I_{11}' over k_1 and k_2

The integration over k_1 for I_{11}' is defined as

$$\begin{aligned}\mathrm{II}_1' &= \frac{-i}{16\pi^2}x_2(1-x_1-x_2)\int \frac{d^4k_1}{(2\pi)^4} \\ &\quad \times \frac{[g^{\alpha\mu} - k_1^\alpha k_1^\mu / m_W^2]}{(k_1^2 - m_W^2)(k_1^2 - m_b^2)[(k_1+k_2)^2 - m_\rho^2]}\frac{2g_{\mu\nu}}{(m_x'^2)^2},\end{aligned} \tag{A45}$$

where the integration measure over the Feynman parameters x_j and s_i are suppressed. The combination of the denominator factors introduces the Feynman parameters z_i $(i = 1, \ldots 3)$, which leads to

$$\begin{aligned}\mathrm{II}_1' &= \frac{-i}{16\pi^2}\frac{x_2(1-x_1-x_2)}{x_1^2(1-x_1)^2}\Gamma(5) \\ &\quad \times \int \prod_{j=1}^3 dz_j \frac{2z_1[g_\nu^\alpha - k_1^\alpha k_{1\nu}/m_W^2]}{D'^5},\end{aligned} \tag{A46}$$

where

$$D' = z_1\left[k_1^2 + \frac{2x_1x_2}{x_1(1-x_1)}k_1\cdot k_2 + \frac{x_2(1-x_2)}{x_1(1-x_1)}k_2^2 - \frac{m_\sigma^2}{x_1(1-x_1)}\right] + z_2[(k_1+k_2)^2 - m_\rho^2] + z_3(k_1^2 - m_W^2) + (1-z_1-z_2-z_3)(k_1^2 - m_b^2). \tag{A47}$$

After the internal momentum translation $k_1 \to k_1 - c_2k_2$, where $c_2 = [x_2z_1 + (1-x_1)z_2]/(1-x_1)$, we can integrate out k_1, resulting in

$$\mathrm{II}'_1 = \frac{1}{(16\pi^2)^2}\int\prod_{j=1}^{3}dz_j\frac{x_2(1-x_1-x_2)z_1}{x_1^2(1-x_1)^2} \times\left\{\frac{4(g_\nu^\alpha - c_2^2k_2^\alpha k_{2\nu}/m_W^2)}{B_2^3[k_2^2-\Delta']^3} - \frac{1}{m_W^2}\frac{g_\nu^\alpha}{B_2^2[k_2^2-\Delta']^2}\right\}, \tag{A48}$$

where B_2 is defined in Eq. (A14) and

$$\Delta' = \frac{z_2}{B_2}m_\rho^2 + \frac{z_3}{B_2}m_W^2 + \frac{1-z_1-z_2-z_3}{B_2}m_b^2 + \frac{z_1m_\sigma}{B_2x_1(1-x_1)}. \tag{A49}$$

We now turn to the integration over k_2,

$$\mathrm{III}'_1 = \frac{1}{(16\pi^2)^2}\frac{x_2(1-x_1-x_2)z_1}{x_1^2(1-x_1)^2} \times\int\frac{d^4k_2}{(2\pi)^4}\frac{(g^{\beta\nu} - k_2^\beta k_2^\nu/m_W^2)}{(k_2^2-m_W^2)(k_2^2-m_a^2)} \times\left\{\frac{4(g_\nu^\alpha - c_2^2k_2^\alpha k_{2\nu}/m_W^2)}{B_2^3[k_2^2-\Delta']^4} - \frac{1}{m_W^2}\frac{g_\nu^\alpha}{B_2^2[k_2^2-\Delta']^3}\right\}, \tag{A50}$$

where the integration measures for the Feynman parameters are also suppressed. The integration over k_2 can be performed with the help of the Feynman parameters y_i,

$$\begin{aligned}\mathrm{III}'_1 &= \frac{1}{(16\pi^2)^2}\frac{x_2(1-x_1-x_2)z_1}{x_1^2(1-x_1)^2}\int dy_1dy_2\int\frac{d^4k_2}{(2\pi)^4}(g^{\beta\nu} - k_2^\beta k_2^\nu/m_W^2)\left\{\frac{\Gamma(5)}{\Gamma(3)}\frac{4y_1^2}{B_2^3}\frac{(g_\nu^\alpha - c_2^2k_2^\alpha k_{2\nu}/m_W^2)}{(k_2^2 - [m_\rho^2\Sigma']/[B_2x_1(1-x_1)])^5}\right.\\ &\quad\left. - \Gamma(4)\frac{y_1}{m_W^2B_2^2}\frac{g_\nu^\alpha}{(k_2^2 - [m_\rho^2\Sigma']/[B_2x_1(1-x_1)])^4}\right\}\\ &= \frac{-i}{(16\pi^2)^3}[x_2(1-x_1-x_2)z_1]\frac{g^{\alpha\beta}}{4}\left\{y_1^2\left[\frac{16x_1(1-x_1)}{m_\rho^6\Sigma'^3} + \frac{4(c_2^2+1)}{m_W^2m_\rho^4B_2\Sigma'^2} + \frac{12c_2^2}{m_W^4m_\rho^2B_2^2x_1(1-x_1)\Sigma'}\right]\right.\\ &\quad\left. + y_1\left[\frac{4}{m_W^2m_\rho^4\Sigma'^2} + \frac{2}{m_W^4m_\rho^2B_2x_1(1-x_1)\Sigma'}\right]\right\},\end{aligned} \tag{A51}$$

where

$$\Sigma' = x_1(1-x_1)\left[y_1z_2 + (y_1z_3 + y_2B_2)\frac{m_W^2}{m_\rho^2} + y_1(1-z_1-z_2-z_3)\frac{m_b^2}{m_\rho^2} + (1-y_1-y_2)B_2\frac{m_a^2}{m_\rho^2}\right] + y_1z_1\frac{m_\sigma^2}{m_\rho^2}. \tag{A52}$$

c. Integration of I'_{12} over k_1 and k_2

The integration over k_1 for I'_{12} is defined as

$$\mathrm{II}'_2 = \frac{-i}{16\pi^2}x_2(1-x_1-x_2)\int\frac{d^4k_1}{(2\pi)^4}\frac{(g^{\alpha\mu} - k_1^\alpha k_1^\mu/m_W^2)}{(k_1^2-m_W^2)(k_1^2-m_b^2)[(k_1+k_2)^2-m_\rho^2]}\frac{2N_{\mu\nu}}{(m_x'^2)^3}. \tag{A53}$$

With the same Feynman parameters z_i as that in Eq. (A11) and the same internal momentum shift $k_1 \to k_1 - c_2k_2$, II'_2 can be transformed into

$$\mathrm{II}'_2 = \frac{i}{16\pi^2}\frac{x_2(1-x_1-x_2)}{x_1^3(1-x_1)^3}\Gamma(6)z_1^3\int\frac{d^4k_1}{(2\pi)^4}\frac{N_\nu'^\alpha}{D'^6}, \tag{A54}$$

where D' is defined in Eq. (A47) and $N_\nu'^\alpha$ is the same as that in Eqs. (A22) and (A23). The integral over k_1 can be worked out with the result given by

$$\mathrm{II}_2' = \frac{1}{(16\pi^2)^2}\frac{x_2(1-x_1x_2)z_1^2}{x_1^3(1-x_1)^3}\left\{-\frac{6d_1d_2k_2^\alpha k_{2\nu}}{B_2^4[k_2^2-\Delta']^4}+\frac{6d_1d_2c_2^2k_2^2k_2^\alpha k_{2\nu}}{B_2^4m_W^2[k_2^2-\Delta']^4}-\frac{(1-2x_1)(2x_1)g_\nu^\alpha}{B_2^3[k_2^2-\Delta']^3}\right.$$
$$+\frac{(1-2x_1)(2x_1)c_2^2k_{2\nu}k_2^\alpha}{B_2^3m_W^2[k_2^2-\Delta']^3}+\frac{(1-2x_1)d_2c_2k_{2\nu}k_2^\alpha}{B_2^3m_W^2[k_2^2-\Delta']^3}+\frac{4(1-2x_1)d_2c_2k_{2\nu}k_2^\alpha}{B_2^3m_W^2[k_2^2-\Delta']^3}$$
$$\left.+\frac{(2x_1)d_1c_2g_\nu^\alpha k_2^2}{B_2^3m_W^2[k_2^2-\Delta']^3}+\frac{(2x_1)d_1c_2k_{2\nu}k_2^\alpha}{B_2^3m_W^2[k_2^2-\Delta']^3}+\frac{d_1d_2k_{2\nu}k_2^\alpha}{B_2^3m_W^2[k_2^2-\Delta']^3}+\frac{3(1-2x_1)(2x_1)g_\nu^\alpha}{2B_2^2m_W^2[k_2^2-\Delta']^2}\right\}. \tag{A55}$$

On the basis of II_2', we can write down the expression for the integration over k_2 by appending the rest propagators, and perform the Feynman parametrization with y_i as that in Eq. (A51) to transform the expression into

$$\mathrm{III}_2' = \int\frac{d^4k_2}{(2\pi)^4}\frac{(g^{\beta\nu}-k_2^\beta k_2^\nu/m_W^2)}{(k_2^2-m_W^2)(k_2^2-m_a^2)}\mathrm{II}_2'$$
$$=\frac{1}{(16\pi^2)^2}\frac{x_2(1-x_1-x_2)z_1^2}{x_1^3(1-x_1)^3}\int\frac{d^4k_2}{(2\pi)^4}\left\{-\frac{\Gamma(6)d_1d_2y_1^3}{B_2^4}\frac{k_2^\alpha k_2^\beta(1-k_2^2/m_W^2)}{[k_2^2-(m_\rho^2\Sigma')/(x_1(1-x_1)B_2)]^6}\right.$$
$$+\frac{\Gamma(6)d_1d_2c_2^2y_1^3}{B_2^4m_W^2}\frac{k_2^\alpha k_2^\beta k_2^2(1-k_2^2/m_W^2)}{[k_2^2-(m_\rho^2\Sigma')/(x_1(1-x_1)B_2)]^6}-\frac{\Gamma(5)(1-2x_1)(2x_1)y_1^2}{\Gamma(3)B_2^3}\frac{(g^{\alpha\beta}-k_2^\alpha k_2^\beta/m_W^2)}{[k_2^2-(m_\rho^2\Sigma')/(x_1(1-x_1)B_2)]^5}$$
$$+\frac{\Gamma(5)(1-2x_1)(2x_1)c_2^2y_1^2}{\Gamma(3)B_2^3m_W^2}\frac{k_2^\alpha k_2^\beta(1-k_2^2/m_W^2)}{[k_2^2-(m_\rho^2\Sigma')/(x_1(1-x_1)B_2)]^5}+\frac{\Gamma(5)(1-2x_1)d_2c_2y_1^2}{\Gamma(3)B_2^3m_W^2}\frac{k_2^\alpha k_2^\beta(1-k_2^2/m_W^2)}{[k_2^2-(m_\rho^2\Sigma')/(x_1(1-x_1)B_2)]^5}$$
$$+\frac{4\Gamma(5)(1-2x_1)d_2c_2y_1^2}{\Gamma(3)B_2^3m_W^2}\frac{k_2^\alpha k_2^\beta(1-k_2^2/m_W^2)}{[k_2^2-(m_\rho^2\Sigma')/(x_1(1-x_1)B_2)]^5}+\frac{\Gamma(5)(2x_1)d_1c_2y_1^2}{\Gamma(3)B_2^3m_W^2}\frac{k_2^2(g^{\alpha\beta}-k_2^\alpha k_2^\beta/m_W^2)}{[k_2^2-(m_\rho^2\Sigma')/(x_1(1-x_1)B_2)]^5}$$
$$+\frac{\Gamma(5)(2x_1)d_1c_2y_1^2}{\Gamma(3)B_2^3m_W^2}\frac{k_2^\alpha k_2^\beta(g^{\alpha\beta}-k_2^2/m_W^2)}{[k_2^2-(m_\rho^2\Sigma')/(x_1(1-x_1)B_2)]^5}+\frac{\Gamma(5)d_1d_2y_1^2}{\Gamma(3)B_2^3m_W^2}\frac{k_2^\alpha k_2^\beta(1-k_2^2/m_W^2)}{[k_2^2-(m_\rho^2\Sigma')/(x_1(1-x_1)B_2)]^5}$$
$$\left.+\frac{9(1-2x_1)(2x_1)y_1}{B_2^2m_W^2}\frac{g^{\alpha\beta}-k_2^\alpha k_2^\beta/m_W^2}{[k_2^2-(m_\rho^2\Sigma')/(x_1(1-x_1)B_2)]^4}\right\}. \tag{A56}$$

Finally, the integration over k_2 results in

$$\mathrm{III}_2' = \frac{i}{(16\pi^2)^3}[x_2(1-x_1-x_2)z_1^2]\frac{g^{\alpha\beta}}{4}\left\{d_1d_2y_1^3\left(\frac{4}{B_2\Sigma'^3m_\rho^6}+\frac{6}{x_1(1-x_1)B_2^2\Sigma'^2m_\rho^4m_W^2}\right)\right.$$
$$+d_1d_2c_2^2y_1^3\left(\frac{6}{x_1(1-x_1)B_2^2\Sigma'^2m_\rho^4m_W^2}+\frac{24}{x_1^2(1-x_1)^2B_2^3\Sigma'm_\rho^2m_W^4}\right)+(2x_1)(1-2x_1)y_1^2\left(\frac{4}{\Sigma'^3m_\rho^6}+\frac{1}{x_1(1-x_1)B_2\Sigma'^2m_\rho^4m_W^2}\right)$$
$$+(2x_1)(1-2x_1)c_2^2y_1^2\left(\frac{1}{x_1(1-x_1)B_2\Sigma'^2m_\rho^4m_W^2}+\frac{3}{x_1^2(1-x_1)^2B_2^2\Sigma'm_\rho^2m_W^4}\right)$$
$$+(1-2x_1)d_2c_2y_1^2\left(\frac{1}{x_1(1-x_1)B_2\Sigma'^2m_\rho^4m_W^2}+\frac{3}{x_1^2(1-x_1)^2B_2^2\Sigma'm_\rho^2m_W^4}\right)$$
$$+(1-2x_1)d_2c_2y_1^2\left(\frac{4}{x_1(1-x_1)B_2\Sigma'^2m_\rho^4m_W^2}+\frac{12}{x_1^2(1-x_1)^2B_2^2\Sigma'm_\rho^2m_W^4}\right)$$
$$+(2x_1)d_1c_2y_1^2\left(\frac{4}{x_1(1-x_1)B_2\Sigma'^2m_\rho^4m_W^2}+\frac{3}{x_1^2(1-x_1)^2B_2^2\Sigma'm_\rho^2m_W^4}\right)$$
$$+(2x_1)d_1c_2y_1^2\left(\frac{1}{x_1(1-x_1)B_2\Sigma'^2m_\rho^4m_W^2}+\frac{3}{x_1^2(1-x_1)^2B_2^2\Sigma'm_\rho^2m_W^4}\right)$$
$$+d_1d_2y_1^2\left(\frac{1}{x_1(1-x_1)B_2\Sigma'^2m_\rho^4m_W^2}+\frac{3}{x_1^2(1-x_1)^2B_2^2\Sigma'm_\rho^2m_W^4}\right)$$
$$\left.+(1-2x_1)(2x_1)y_1\left(\frac{6}{x_1(1-x_1)\Sigma'^2m_\rho^4m_W^2}+\frac{3}{x_1^2(1-x_1)^2B_2\Sigma'm_\rho^2m_W^4}\right)\right\}. \tag{A57}$$

3. Final results

The final analytic formula for $\mathcal{I}'_2$ is obtained by summing up those for III'_1 and III'_2, given by

$$\mathcal{I}'_2 = \frac{1}{2}(16\pi^2)^3 m_\rho^4 m_W^4 \gamma_\beta \gamma_\alpha (\mathrm{III}'_1 + \mathrm{III}'_2) = \frac{i}{2}\left(\frac{m_W^4}{m_\rho^4}\mathcal{I}'_{22} + \frac{m_W^2}{m_\rho^2}\mathcal{I}'_{21} + \mathcal{I}'_{20}\right), \tag{A58}$$

where

$$\mathcal{I}'_{20} = \frac{x_2(1-x_1-x_2)z_1}{\Sigma'^3}\left\{-16x_1(1-x_1)y_1^2 + \frac{4d_1 d_2 y_1^3 z_1}{B_2} + 4(1-2x_1)(2x_1)y_1^2 z_1\right\}, \tag{A59}$$

$$\begin{aligned}\mathcal{I}'_{21} = &-\frac{x_2(1-x_1-x_2)z_1}{\Sigma'^2}\left\{\frac{4y_1^2(c_2^2+1)}{B_2} + 4y_1\right\} + \frac{x_2(1-x_1-x_2)z_1^2}{x_1(1-x_1)\Sigma'^2}\left\{\frac{6d_1 d_2 y_1^3}{B_2^2}\right.\\ &+ \frac{6d_1 d_2 c_2^2 y_1^3}{B_2^2} + \frac{(1-2x_1)(2x_1)y_1^2}{B_2} + \frac{(1-2x_1)(2x_1)c_2^2 y_1^2}{B_2} + \frac{(1-2x_1)d_2 c_2 y_1^2}{B_2}\\ &\left.+ \frac{4(1-2x_1)d_2 c_2 y_1^2}{B_2} + \frac{4(2x_1)d_1 c_2 y_1^2}{B_2} + \frac{(2x_1)d_1 c_2 y_1^2}{B_2} + \frac{d_1 d_2 y_1^2}{B_2} + 6(1-2x_1)(2x_1)y_1\right\},\end{aligned} \tag{A60}$$

$$\begin{aligned}\mathcal{I}'_{22} = &-\frac{x_2(1-x_1-x_2)z_1}{x_1(1-x_1)\Sigma'}\left\{\frac{12y_1^2 c_2^2}{B_2^2} + \frac{2y_1}{B_2}\right\} + \frac{x_2(1-x_1-x_2)z_1^2}{x_1^2(1-x_1)^2\Sigma'}\left\{\frac{24d_1 d_2 c_2^2 y_1^3}{B_2^3}\right.\\ &+ \frac{3(1-2x_1)(2x_1)c_2^2 y_1^2}{B_2^2} + \frac{3(1-2x_1)d_2 c_2 y_1^2}{B_2^2} + \frac{12(1-2x_1)d_2 c_2 y_1^2}{B_2^2} + \frac{3(2x_1)d_1 c_2 y_1^2}{B_2^2}\\ &\left.+ \frac{3(2x_1)d_1 c_2 y_1^2}{B_2^2} + \frac{3d_1 d_2 y_1^2}{B_2^2} + \frac{3(1-2x_1)(2x_1)y_1}{B_2}\right\}.\end{aligned} \tag{A61}$$

Note that the nine-dimensional integration measure for the Feynman parameters x_i, y_i, z_i previously suppressed is defined by

$$\text{measure} = \int_0^1 ds_2 \int_0^1 ds_3 \int_0^1 dx_1 \int_0^{1-x_1} dx_2 \int_0^1 dy_1 \int_0^{1-y_1} dy_2 \int_0^1 dz_1 \int_0^{1-z_1} dz_2 \int_0^{1-z_1-z_2} dz_3. \tag{A62}$$

As mentioned before, $\mathcal{I}''_2$ can be simply obtained by exchanging the charged scalar masses $m_{H_1} \leftrightarrow m_{H_2}$ in Eq. (A58). This completes our analytical derivation of the integral $\mathcal{I}_2$.

For the remaining nine-dimensional Feynman parameter integrations in $\mathcal{I}_2$, we also use the three packages as in the κ_2 part calculation: MATHEMATICA (Global Adaptive), SECDEC-2.1.4 [11], and VEGAS in GSL [12], in order to make a cross-check. Consequently, all of them give essentially the same result within errors. For the particle spectrum of the benchmark point listed in Eq. (A32), the three-loop integration $\mathcal{I}_2$ is given by

$$\mathcal{I}_2 = 4.15i. \tag{A63}$$

Together with $\mathcal{I}_1 = 2.16i$ as calculated in the previous section, we can predict the neutrino mass matrix numerically by taking various possible values of ξ, and our results are given by

$$\xi = 0.5: \qquad m_\nu = \begin{pmatrix} \mathcal{O}(10^{-3}) & \mathcal{O}(10^{-3}) & 1.52 \\ \mathcal{O}(10^{-3}) & 3.14 & 4.74 \\ 1.52 & 4.74 & 4.42 \end{pmatrix} \times 10^{-13}\ \text{GeV}, \tag{A64}$$

$$\xi = 0.8: \qquad m_\nu = \begin{pmatrix} \mathcal{O}(10^{-3}) & \mathcal{O}(10^{-3}) & 1.81 \\ \mathcal{O}(10^{-3}) & 3.74 & 5.64 \\ 1.81 & 5.64 & 5.25 \end{pmatrix} \times 10^{-13}\ \text{GeV}, \tag{A65}$$

$$\xi = 1: \qquad m_\nu = \begin{pmatrix} \mathcal{O}(10^{-3}) & \mathcal{O}(10^{-3}) & 2.00 \\ \mathcal{O}(10^{-3}) & 4.13 & 6.23 \\ 2.00 & 6.23 & 5.80 \end{pmatrix} \times 10^{-13}\ \mathrm{GeV}, \tag{A66}$$

$$\xi = 5: \qquad m_\nu = \begin{pmatrix} \mathcal{O}(10^{-3}) & \mathcal{O}(10^{-3}) & 5.80 \\ \mathcal{O}(10^{-3}) & 12.0 & 18.1 \\ 5.80 & 18.1 & 16.9 \end{pmatrix} \times 10^{-13}\ \mathrm{GeV}. \tag{A67}$$

Note that Eq. (A67) can be regarded as the extreme case allowed by the naturalness argument [13]. In summary, we see that the predicted neutrino mass matrix elements are typically smaller than the realistic values up to 2 orders of magnitude for the benchmark point shown in the first version of Ref. [10] before the publication of its erratum.

[1] Y. Fukuda *et al.* (Super-Kamiokande Collaboration), Phys. Rev. Lett. **81**, 1562 (1998); Q. R. Ahmad *et al.* (SNO Collaboration), Phys. Rev. Lett. **89**, 011301 (2002); K. Eguchi *et al.* (KamLAND Collaboration), Phys. Rev. Lett. **90**, 021802 (2003); F. P. An *et al.* (DAYA-BAY Collaboration), Phys. Rev. Lett. **108**, 171803 (2012); J. K. Ahn *et al.* (RENO Collaboration), Phys. Rev. Lett. **108**, 191802 (2012); K. Abe *et al.* (T2K Collaboration), Phys. Rev. Lett. **112**, 061802 (2014).

[2] K. G. Begeman, A. H. Broeils, and R. H. Sanders, Mon. Not. R. Astron. Soc. **249**, 523 (1991).

[3] P. A. R. Ade *et al.* (Planck Collaboration), arXiv:1303.5076 [Astron. Astrophys. (to be published)].

[4] D. Clowe, M. Bradac, A. H. Gonzalez, M. Markevitch, S. W. Randall, C. Jones, and D. Zaritsky, Astrophys. J. **648**, L109 (2006).

[5] P. Minkowski, Phys. Lett. **67B**, 421 (1977); M. Gell-Mann, P. Ramond, and R. Slansky in *Supergravity*, edited by F. Nieuwenhuizen and D. Friedman (North Holland, Amsterdam, 1979), p. 315; T. Yanagida, in *Workshop on Unified Theories and the Baryon Number of the Universe*, edited by O. Sawada and A. Sugamoto (KEK, Japan, 1979); Prog. Theor. Phys. **64**, 1103 (1980); S. L. Glashow, in *Proc. of the Cargese Summer Institute on Quarks and Leptons, Cargese, 1979*, edited by M. Levy *et al.* (Plenum, New York, 1980), p. 707; R. N. Mohapatra and G. Senjanovic, Phys. Rev. Lett. **44**, 912 (1980).

[6] J. Schechter and J. W. F. Valle, Phys. Rev. D **22**, 2227 (1980); T. P. Cheng and L. F. Li, Phys. Rev. D **22**, 2860 (1980); M. Magg and C. Wetterich, Phys. Lett. **94B**, 61 (1980); C. Wetterich, Nucl. Phys. **B187**, 343 (1981); G. Lazarides, Q. Shafi, and C. Wetterich, Nucl. Phys. **B181**, 287 (1981); R. N. Mohapatra and G. Senjanovic, Phys. Rev. D **23**, 165 (1981).

[7] R. Foot, H. Lew, X. G. He, and G. C. Joshi, Z. Phys. C **44**, 441 (1989); E. Ma, Phys. Rev. Lett. **81**, 1171 (1998).

[8] A. Zee, Phys. Lett. **93B**, 389 (1980); **95B**, 461 (1980); A. Zee, Nucl. Phys. **B264**, 99 (1986); K. S. Babu, Phys. Lett. B **203**, 132 (1988).

[9] L. M. Krauss, S. Nasri, and M. Trodden, Phys. Rev. D **67**, 085002 (2003); E. Ma, Phys. Rev. D **73**, 077301 (2006); M. Aoki, S. Kanemura, and O. Seto, Phys. Rev. Lett. **102**, 051805 (2009).

[10] M. Gustafsson, J. M. No, and M. A. Rivera, Phys. Rev. Lett. **110**, 211802 (2013); **112**, 259902(E) (2014).

[11] J. Carter and G. Heinrich, Comput. Phys. Commun. **182**, 1566 (2011).

[12] http://www.gnu.org/software/gsl/.

[13] M. Nebot, J. F. Oliver, D. Palao, and A. Santamaria, Phys. Rev. D **77**, 093013 (2008).

[14] K. A. Olive *et al.* (Particle Data Group), Chin. Phys. C **38**, 090001 (2014).

[15] H. Pas, M. Hirsch, H. V. Klapdor-Kleingrothaus, and S. G. Kovalenko, Phys. Lett. B **498**, 35 (2001).

[16] F. F. Deppisch, M. Hirsch, and H. Pas, J. Phys. G **39**, 124007 (2012).

[17] C. S. Chen, C. Q. Geng, and J. N. Ng, Phys. Rev. D **75**, 053004 (2007); C. S. Chen, C. Q. Geng, J. N. Ng, and J. M. S. Wu, J. High Energy Phys. 08 (2007) 022.

[18] M. Gustafsson, J. M. No, and M. A. Rivera, Phys. Rev. D **90**, 013012 (2014).

[19] S. F. King, A. Merle, and L. Panizzi, arXiv:1406.4137.

[20] M. Doi, T. Kotani, and E. Takasugi, Prog. Theor. Phys. Suppl. **83**, 1 (1985).

[21] J. Suhonen and O. Civitarese, Phys. Rep. **300**, 123 (1998).

[22] M. Agostini *et al.* (GERDA Collaboration), Phys. Rev. Lett. **111**, 122503 (2013).

[23] A. Gando *et al.* (KamLAND-Zen Collaboration), Phys. Rev. C **85**, 045504 (2012); Phys. Rev. Lett. **110**, 062502 (2013).

[24] J. Argyriades *et al.* (NEMO Collaboration), Phys. Rev. C **80**, 032501 (2009).

[25] C. Arnaboldi *et al.* (CUORICINO Collaboration), Phys. Rev. C **78**, 035502 (2008).

[26] R. Arnold *et al.* (NEMO Collaboration), Phys. Rev. Lett. **95**, 182302 (2005).

[27] A. S. Barabash, and V. B. Brudanin (NEMO Collaboration), Phys. At. Nucl. **74**, 312 (2011).

[28] S. Schonert *et al.* (GERDA Collaboration), Nucl. Phys. B, Proc. Suppl. **145**, 242 (2005); R. Gaitskell *et al.* (Majorana Collaboration), arXiv:nucl-ex/0311013; J. J. Gomez-Cadenas, J. Martin-Albo, and F. Monrabal, JINST **7**, C11007 (2012); J. J. Gomez-Cadenas, J. Martin-Albo, M. Mezzetto, F. Monrabal, and M. Sorel, Riv. Nuovo Cimento **35**, 29 (2012); R. Arnold *et al.* (SuperNEMO Collaboration), Eur. Phys. J. C **70**, 927 (2010); J. Maneira (SNO+ Collaboration), J. Phys. Conf. Ser. **447**, 012065 (2013); C. Arnaboldi *et al.* (CUORE Collaboration), Nucl. Instrum. Methods Phys. Res., Sect. A **518**, 775 (2004); R. Ardito, C. Arnaboldi, D. R. Artusa, F. T. Avignone III, M. Balata, I. Bandac, M. Barucci, and J. W. Beeman *et al.*, arXiv:hep-ex/0501010.

[29] J. Adam *et al.* (MEG Collaboration), Phys. Rev. Lett. **110**, 201801 (2013).

[30] K. Hayasaka *et al.* (Belle Collaboration), Phys. Lett. B **687**, 139 (2010).

[31] W. Grimus, L. Lavoura, O. M. Ogreid, and P. Osland, Nucl. Phys. **B801**, 81 (2008).

[32] M. Baak, M. Goebel, J. Haller, A. Hoecker, D. Kennedy, R. Kogler, K. Moenig, and M. Schott, and J. Stelzer, Eur. Phys. J. C **72**, 2205 (2012).

[33] R. Barbieri, L. J. Hall, and V. S. Rychkov, Phys. Rev. D **74**, 015007 (2006); L. Lopez Honorez, E. Nezri, J. F. Oliver, and M. H. G. Tytgat, J. Cosmol. Astropart. Phys. 02 (2007) 028.

[34] A. Arhrib, Y.-L. S. Tsai, Q. Yuan, and T.-C. Yuan, J. Cosmol. Astropart. Phys. 06 (2014) 030.

[35] M. Gustafsson, S. Rydbeck, L. Lopez-Honorez, and E. Lundstrom, Phys. Rev. D **86**, 075019 (2012).

[36] T. Hambye, F.-S. Ling, L. Lopez Honorez, and J. Rocher, J. High Energy Phys. 07 (2009) 090; 05 (2010) 066.

[37] G. Belanger, B. Dumont, U. Ellwanger, J. F. Gunion, and S. Kraml, Phys. Rev. D **88**, 075008 (2013).

[38] E. Lundstrom, M. Gustafsson, and J. Edsjo, Phys. Rev. D **79**, 035013 (2009).

[39] A. Pierce and J. Thaler, J. High Energy Phys. 08 (2007) 026.

[40] G. Aad *et al.* (ATLAS Collaboration), J. High Energy Phys. 04 (2014) 169.

[41] G. Aad *et al.* (ATLAS Collaboration), J. High Energy Phys. 05 (2014) 071.

[42] G. Aad *et al.* (ATLAS Collaboration), J. High Energy Phys. 10 (2014) 96.

[43] V. Khachatryan *et al.* (CMS Collaboration), Eur. Phys. J. C **74**, 3036 (2014).

[44] V. Khachatryan *et al.* (CMS Collaboration), Phys. Rev. D **90**, 092007 (2014).

[45] G. Aad *et al.* (ATLAS Collaboration), Eur. Phys. J. C **72**, 2244 (2012).

[46] S. Chatrchyan *et al.* (CMS Collaboration), Eur. Phys. J. C **72**, 2189 (2012).